A full analytic solution of SO(10)-inspired leptogenesis

JHEP

Published for SISSA by Springer

Received: May 22, 2017
Revised: September 3, 2017
Accepted: September 7, 2017
Published: October 4, 2017

A full analytic solution of SO(10)-inspired leptogenesis

Pasquale Di Bari[a] **and Michele Re Fiorentin**[a,b]

[a] *Physics and Astronomy, University of Southampton, Southampton, SO17 1BJ, U.K.*

[b] *Center for Sustainable Future Technologies, Istituto Italiano di Tecnologia, corso Trento 21, 10129 Torino, Italy*

E-mail: P.Di-Bari@soton.ac.uk, michele.refiorentin@iit.it

Abstract: Recent encouraging experimental results on neutrino mixing parameters prompt further investigation on SO(10)-inspired leptogenesis and on the associated strong thermal solution that has correctly predicted a non-vanishing reactor mixing angle, it further predicts $\sin\delta \lesssim 0$, now supported by recent results at $\sim 95\%$ C.L., normally ordered neutrino masses and atmospheric mixing angle in the first octant, best fit results in latest global analyses. Extending a recent analytical procedure, we account for the mismatch between the Yukawa basis and the weak basis, that in SO(10)-inspired models is described by a CKM-like unitary transformation V_L, obtaining a full analytical solution that provides useful insight and reproduces accurately all numerical results, paving the way for future inclusion of different sources of theoretical uncertainties and for a statistical analysis of the constraints. We show how muon-dominated solutions appear for large values of the lightest neutrino mass in the range (0.01–1) eV but also how they necessarily require a mild fine tuning in the seesaw relation. For the dominant (and untuned) tauon-dominated solutions we show analytically how, turning on $V_L \simeq V_{\rm CKM}$, some of the constraints on the low energy neutrino parameters get significantly relaxed. In particular we show how the upper bound on the atmospheric neutrino mixing angle in the strong thermal solution gets relaxed from $\theta_{23} \lesssim 41^\circ$ to $\theta_{23} \lesssim 44^\circ$, an important effect in the light of the most recent NOνA, T2K and IceCube results.

Keywords: Beyond Standard Model, Cosmology of Theories beyond the SM, CP violation, Neutrino Physics

ArXiv ePrint: 1705.01935

https://doi.org/10.1007/JHEP10(2017)029

JHEP10(2017)029

Contents

JHEP10(2017)029

1 Introduction

The latest results from the LHC show no evidence for new physics at the TeV scale. Analogously, negative results also come from direct dark matter, cLFV and electric dipole moments searches. Potential manifestations of new physics are given by the long standing muon $g-2$ anomaly and by the recent anomalies reported in B decays [1] but more solid evidence is required and they are indeed currently regarded as anomalies. On the other hand robust motivations for extending the Standard Model come from neutrino masses and mixing and from the cosmological puzzles. In the absence of new physics at the TeV scale or below, it is reasonable to think that their solution is related to the existence of higher energy scales. In particular a combined explanation of neutrino masses and mixing, from a conventional high energy type I seesaw mechanism [2–7], and of the matter-antimatter asymmetry of the Universe from (consequentially high energy scale) leptogenesis [8], should be currently regarded as the simplest and attractive possibility.

Interestingly, latest neutrino oscillation experiments global analyses also seem to support *CP* violation in left-handed (LH) neutrino mixing (at 95% C.L. in [9] and at 70% C.L. in [10]). Though this is not a sufficient condition for the existence of a source of *CP* violation for successful leptogenesis, if confirmed, it would be still an important result since it would make quite plausible the presence of *CP* violation also in heavy right-handed (RH) neutrino mixing, the natural dominant source of *CP* violation for leptogenesis (barring special scenarios).[1] In addition, the exclusion of quasi-degenerate light neutrino masses can

[1] Conversely, *CP* conservation in LH neutrino mixing would legitimately cast some doubts on it.

be also regarded as a positive experimental outcome for minimal scenarios of leptogenesis, based on type I seesaw mechanism and thermal RH neutrino production, since the bulk of solutions requires values of neutrino masses $m_i \lesssim \mathcal{O}(0.1)\,\text{eV}$ [11–16], even when charged lepton [17, 18] and heavy neutrino [19] flavour effects are taken into account.[2] Therefore, this current phenomenological picture certainly encourages further investigation on high energy scale scenarios of leptogenesis.

On the other hand the possibility to test more stringently leptogenesis and even have any hope to prove it, seems necessarily to rely on the identification of specific scenarios, possibly emerging from well motivated theoretical frameworks. This is in order to reduce the number of independent parameters, increasing the predictive power and over-constraining the seesaw parameter space. The sharper the predictions are, the lower the probability that these are just a mere coincidence. This challenging strategy has been strongly boosted by the measurement of a non-vanishing value of the reactor mixing angle, sufficiently large to make possible the measurements of the unknown parameters in the leptonic mixing matrix: *CP* violating Dirac phase, neutrino mass ordering and a determination of the deviation of the atmospheric mixing angle from the maximal value.

The latest results from the NOνA long baseline experiment favour a $\sim 5^\circ$ deviation of the atmospheric mixing angle from maximal mixing [20], while the results from the T2K long baseline experiment [21] and from the IceCube neutrino detector [22] do not find evidence of such deviation so far, so that a mild tension exists but still within 90% C.L. At the same time both experiments strengthen the support for negative values of $\sin\delta$. Moreover they also show an emergence for a slight preference for normally ordered neutrino masses. When all results are combined, two recent global analyses find that first octant for atmospheric mixing angle with normally ordered neutrino masses (NO) emerges as a best fit solution, though the preference over inverted ordered neutrino masses (IO), allowing both first and second octant, is currently slight, at the level of $\sim 1.7\,\sigma$ [9] or even less [10].

Intriguingly, this emerging potential experimental set of results for the unknown neutrino oscillation parameters nicely supports the expectations from the so called strong thermal SO(10)-inspired leptogenesis solution [23], indeed strictly requiring NO, atmospheric mixing angle in the first octant and favouring negative values of $\sin\delta$ for sufficiently large values of the atmospheric mixing angle.[3]

This solution relies on two independent conditions and it is highly non trivial that they can be satisfied simultaneously. The first one, on the model building side, is the SO(10)-*inspired condition* [25–29], and it corresponds to assume that the Dirac neutrino mass matrix is *not too different* from the up-quark mass matrix, a typical feature of different grand-unified models such as SO(10) models.[4] The second assumption is dictated

[2] As we will discuss in detail, muon-dominated solutions in SO(10)-inspired leptogenesis are found for m_i as large as $\sim 1\,\text{eV}$, but these solutions suffer of some fine-tuning, as we will notice, and are certainly less interesting than tauon-dominated solutions representing the bulk of solutions and respecting the upper bound $m_i \lesssim \mathcal{O}(0.1\,\text{eV})$.

[3] The solution also requires non-vanishing θ_{13} for large values of the initial pre-existing asymmetry $N_{B-L}^{\text{p,i}} \gtrsim 0.001$, a result preliminarily presented in [24] before the discovery from nuclear reactors.

[4] As we will see in more detail, even without imposing the strong thermal condition, the SO(10)-inspired condition already strongly favours NO and to less extent the atmospheric mixing angle in the first octant.

JHEP10(2017)029

purely by a cosmological requirement, the independence of the final asymmetry of the initial conditions (the *strong thermal leptogenesis condition*). The latter, in the case of hierarchical RH neutrino mass patterns, is satisfied only for quite a specific case, the tauon N_2-dominated scenario [30] and, as we said, it is highly not trivial that this is realised within SO(10)-inspired models. If future data will confirm NO together with $\sin\delta < 0$ and atmospheric mixing angle in the first octant, the statistical significance of the agreement between theoretical predictions and experimental results would be very interesting, since the probability to find by chance such an agreement with the strong thermal SO(10)-inspired leptogenesis solution is lower than $\sim 5\%$ [23].

A full analytical description of SO(10)-inspired leptogenesis is greatly helpful in different respects. First, it provides a useful analytical insight able to clarify different interesting aspects of SO(10)-inspired leptogenesis, as we will discuss in detail. On more practical grounds, the expected future improvement in the determination of the neutrino mixing parameters clearly calls for an analogous improvement in the theoretical predictions with a reduction of the theoretical uncertainties. To this extent, for an inclusion of more subtle effects in the derivation of the low energy neutrino constraints, a full analytical calculation of the final asymmetry allows a fast generation of solutions, something essential also for a precise statistical derivation of the constraints, so far qualitatively derived just from scatter plots. Driven by these motivations, in this paper we extend the analytic procedure of [31], taking into account the mismatch between the Yukawa basis and the weak basis. This will allow to reproduce with great accuracy all results obtained only numerically so far.[5] The paper is organised as follows. In section 2 we review the seesaw type I mechanism and current neutrino oscillation data. In section 3 we discuss SO(10)-inspired leptogenesis extending the analytical procedure discussed in [31] taking into account the mismatch, described by a unitary matrix V_L, between the Yukawa basis, where the neutrino Dirac mass matrix is diagonal, and the weak basis, where the charged lepton mass matrix is diagonal.[6] In this way we obtain some general results that in section 4 we specialise to reproduce a few different effects governed by the matrix V_L including the application to strong thermal leptogenesis showing how the upper bound on the atmospheric mixing angle gets relaxed. Finally in section 5 we draw the conclusions.

2 Seesaw and low energy neutrino parameters

Augmenting the SM with three RH neutrinos N_{iR} with Yukawa couplings h and a Majorana mass term M, in the flavour basis, where both charged lepton mass matrix m_ℓ and M are diagonal, one can write the leptonic mass terms generated after spontaneous symmetry breaking as ($\alpha = e, \mu, \tau$ and $i = 1, 2, 3$)

$$-\mathcal{L}_M = \overline{\alpha_L}\, D_{m_\ell}\, \alpha_R + \overline{\nu_{\alpha L}}\, m_{D\alpha i}\, N_{iR} + \frac{1}{2}\, \overline{N^c_{iR}}\, D_M\, N_{iR} + \text{h.c.}\,, \tag{2.1}$$

[5] In the paper we will consider a non-supersymmetric framework. For a detailed discussion on the supersymmetric extension we refer the reader to [32], where it has been shown that constraints get significantly relaxed only at large values $\tan\beta \gtrsim 15$. The analytical results that we discuss here can be easily exported to the supersymmetric case.

[6] We summarise in the appendix the set of expressions that allow a full general analytical calculation of the asymmetry in SO(10)-inspired leptogenesis.

JHEP10(2017)029

where $D_{m_\ell} \equiv \mathrm{diag}(m_e, m_\mu, m_\tau)$, $D_M \equiv \mathrm{diag}(M_1, M_2, M_3)$ and m_D is the neutrino Dirac mass matrix. In the seesaw limit, $M \gg m_D$, the mass spectrum splits into two sets of Majorana eigenstates: a light set with masses $m_1 \leq m_2 \leq m_3$ given by the seesaw formula [2–7]

$$D_m = U^\dagger \, m_D \, \frac{1}{D_M} \, m_D^T \, U^\star \,, \tag{2.2}$$

with $D_m = \mathrm{diag}(m_1, m_2, m_3)$, and a heavy set with masses basically coinciding with D_M. The matrix U, which diagonalises the light neutrino mass matrix $m_\nu = -m_D \, M^{-1} \, m_D^T$ in the weak basis, can then be identified with the PMNS lepton mixing matrix. For NO, this can be parameterised in terms of the usual mixing angles θ_{ij}, the Dirac phase δ and the Majorana phases ρ and σ, as

$$U = \begin{pmatrix} c_{12}\, c_{13} & s_{12}\, c_{13} & s_{13}\, e^{-\mathrm{i}\,\delta} \\ -s_{12}\, c_{23} - c_{12}\, s_{23}\, s_{13}\, e^{\mathrm{i}\,\delta} & c_{12}\, c_{23} - s_{12}\, s_{23}\, s_{13}\, e^{\mathrm{i}\,\delta} & s_{23}\, c_{13} \\ s_{12}\, s_{23} - c_{12}\, c_{23}\, s_{13}\, e^{\mathrm{i}\,\delta} & -c_{12}\, s_{23} - s_{12}\, c_{23}\, s_{13}\, e^{\mathrm{i}\,\delta} & c_{23}\, c_{13} \end{pmatrix} \mathrm{diag}\left(e^{i\,\rho}, 1, e^{i\,\sigma}\right) \,. \tag{2.3}$$

For IO, since we are defining $m_1 \leq m_2 \leq m_3$, this should be replaced by the column permuted matrix

$$U^{(\mathrm{IO})} = U^{(\mathrm{NO})} \begin{pmatrix} 0 & 1 & 0 \\ 0 & 0 & 1 \\ 1 & 0 & 0 \end{pmatrix} \,. \tag{2.4}$$

However, in this paper we will focus on the NO case, since IO is only marginally allowed imposing just successful SO(10)-inspired leptogenesis [33][7] and it is completely excluded imposing in addition the strong thermal leptogenesis condition. In the case of NO, latest neutrino oscillation experiments global analyses find for the mixing angles and the leptonic Dirac phase δ, the following best fit values, 1σ errors and 3σ intervals [9]:

$$\begin{aligned} \theta_{13} &= 8.45^\circ \pm 0.15^\circ \quad [8.0^\circ, 9.0^\circ] \,, \\ \theta_{12} &= 33^\circ \pm 1^\circ \quad [30^\circ, 36^\circ] \,, \\ \theta_{23} &= 41^\circ \pm 1^\circ \quad [38^\circ, 51.65^\circ] \,, \\ \delta &= -0.62\pi \pm 0.2\pi \quad [-1.24\pi, 0.17\pi] \,. \end{aligned} \tag{2.5}$$

It is interesting that there is already an excluded interval $\delta \ni [0.17\,\pi, 0.76\pi]$ at $3\,\sigma$ and that $\sin\delta > 0$ is excluded at 2σ favouring $\sin\delta < 0$ (in [10] a lower statistical significance is found). Of course there are no experimental constraints on the Majorana phases. Neutrino oscillation experiments also measure two mass squared differences, finding for the solar neutrino mass scale $m_{\mathrm{sol}} \equiv \sqrt{m_2^2 - m_1^2} = (8.6 \pm 0.1)\,\mathrm{meV}$ and for the atmospheric neutrino mass scale $m_{\mathrm{atm}} \equiv \sqrt{m_3^2 - m_2^2} = (49.5 \pm 0.05)\,\mathrm{meV}$ [9].

There is no signal from neutrinoless double beta ($0\nu\beta\beta$) decay experiments that, therefore, place an upper bound on the effective $0\nu\beta\beta$ neutrino mass defined as

$$m_{ee} \equiv |m_{\nu ee}| = |U_{e1}^2 \, m_1 + U_{e2}^2 \, m_2 + U_{e3}^2 \, m_3| \,. \tag{2.6}$$

[7] It is allowed only at quite large values of $m_1 \gtrsim 10^{-2+0.14\,(52-\theta_{23}/^\circ)}\,\mathrm{meV}$, so that for example using a more aggressive upper bound from the same *Planck* collaboration $\sum_i m_i \lesssim 0.17\,\mathrm{eV}$ [34], translating into $m_1 \lesssim 0.04\,\mathrm{eV}$ for IO, the allowed region is almost completely ruled out.

JHEP10(2017)029

Currently, the most stringent reported upper bound comes from the KamLAND-Zen collaboration finding, at 90% C.L., $m_{ee} \leq (61\text{–}165)\,\text{meV}$ [35], where the range accounts for nuclear matrix element uncertainties.

Cosmological observations place an upper bound on the sum of the neutrino masses. The *Planck* satellite collaboration obtains a robust stringent upper bound $\sum_i m_i \lesssim 230\,\text{meV}$ at 95%C.L. [34] that, taking into account neutrino oscillation experimental determination of the solar and atmospheric neutrino mass scales, translates into an upper bound on the lightest neutrino mass $m_1 \lesssim 70\,\text{meV}$.

3 SO(10)-inspired leptogenesis

The neutrino Dirac mass matrix can be diagonalised (singular value decomposition) as

$$m_D = V_L^\dagger \, D_{m_D} \, U_R \,, \tag{3.1}$$

where $D_{m_D} \equiv \text{diag}(m_{D1}, m_{D2}, m_{D3})$ and where V_L and U_R are the two unitary matrices transforming respectively the LH and RH neutrino fields from the flavour basis (where m_ℓ and M are diagonal) to the Yukawa basis (where m_D is diagonal).

If we parameterise the neutrino Dirac masses m_{Di} in terms of the up quark masses,

$$(m_{D1}, m_{D2}, m_{D3}) = (\alpha_1 \, m_\text{u}, \alpha_2 \, m_\text{c}, \alpha_3 \, m_\text{t}) \,, \tag{3.2}$$

we can impose so called SO(10)-*inspired conditions* defined as:

- $m_{D3} \gg m_{D2} \gg m_{D_1}$, implying $\alpha_i = \mathcal{O}(0.1\text{–}10)$,
- $I \leq V_L \lesssim V_\text{CKM}$.

The latter should be read in a way that parameterising V_L in the same way as the leptonic mixing matrix U, the three mixing angles θ_{12}^L, θ_{23}^L and θ_{13}^L cannot have values much larger than the three mixing angles in the CKM matrix.[8]

Inserting the singular value decomposed form for m_D eq. (3.1) into the seesaw formula eq. (2.2), one obtains

$$M^{-1} \equiv U_R \, D_M \, U_R^T = -D_{m_D}^{-1} \, \widetilde{m}_\nu \, D_{m_D}^{-1} \,, \tag{3.3}$$

where $M \equiv U_R^\star \, D_M \, U_R^\dagger$ and $\widetilde{m}_\nu \equiv V_L \, m_\nu \, V_L^T$ are respectively the Majorana mass matrix and the light neutrino mass matrix in the Yukawa basis. Diagonalising the matrix on the RH side of eq. (3.3), one can express the RH neutrino masses and the RH neutrino mixing matrix U_R in terms of m_ν, V_L and the three α_i.

The analytical procedure discussed in [31], within the approximation $V_L \simeq I$, gets easily generalised for $V_L \neq I$ replacing $m_\nu \to \widetilde{m}_\nu$ [36] and in this case one finds for the

[8] Precisely we adopt: $\theta_{12}^L \leq 13^\circ \simeq \theta_{12}^\text{CKM} \equiv \theta_c$, $\theta_{23}^L \leq 2.4^\circ \simeq \theta_{23}^\text{CKM}$, $\theta_{13}^L \leq 0.2^\circ \simeq \theta_{13}^\text{CKM}$. However, notice that the validity of our analytical solution goes beyond these ranges of values for the mixing angles in the V_L. We will discuss this point in greater detail in the appendix.

JHEP10(2017)029

three RH neutrino masses[9]

$$M_1 \simeq \frac{m_{D1}^2}{|\widetilde{m}_{\nu 11}|}\,, \quad M_2 \simeq \frac{m_{D2}^2}{m_1\, m_2\, m_3}\,\frac{|\widetilde{m}_{\nu 11}|}{|(\widetilde{m}_\nu^{-1})_{33}|}\,, \quad M_3 \simeq m_{D3}^2\,|(\widetilde{m}_\nu^{-1})_{33}|, \tag{3.4}$$

and for the RH neutrino mixing matrix

$$U_R \simeq \begin{pmatrix} 1 & -\frac{m_{D1}}{m_{D2}}\frac{\widetilde{m}^\star_{\nu 12}}{\widetilde{m}^\star_{\nu 11}} & \frac{m_{D1}}{m_{D3}}\frac{(\widetilde{m}_\nu^{-1})^\star_{13}}{(\widetilde{m}_\nu^{-1})^\star_{33}} \\ \frac{m_{D1}}{m_{D2}}\frac{\widetilde{m}_{\nu 12}}{\widetilde{m}_{\nu 11}} & 1 & \frac{m_{D2}}{m_{D3}}\frac{(\widetilde{m}_\nu^{-1})^\star_{23}}{(\widetilde{m}_\nu^{-1})^\star_{33}} \\ \frac{m_{D1}}{m_{D3}}\frac{\widetilde{m}_{\nu 13}}{\widetilde{m}_{\nu 11}} & -\frac{m_{D2}}{m_{D3}}\frac{(\widetilde{m}_\nu^{-1})_{23}}{(\widetilde{m}_\nu^{-1})_{33}} & 1 \end{pmatrix} D_\Phi\,, \tag{3.5}$$

where the three phases in $D_\phi \equiv \mathrm{diag}(e^{-i\frac{\Phi_1}{2}}, e^{-i\frac{\Phi_2}{2}}, e^{-i\frac{\Phi_3}{2}})$ are given by

$$\Phi_1 = \mathrm{Arg}[-\widetilde{m}^\star_{\nu 11}]\,, \quad \Phi_2 = \mathrm{Arg}\left[\frac{\widetilde{m}_{\nu 11}}{(\widetilde{m}_\nu^{-1})_{33}}\right] - 2\,(\rho+\sigma) - 2\,(\rho_L+\sigma_L)\,, \quad \Phi_3 = \mathrm{Arg}[-(\widetilde{m}_\nu^{-1})_{33}]\,. \tag{3.6}$$

It should be noticed how the Majorana phases ρ_L and σ_L enter directly the expression for the RH neutrino Majorana phases (more precisely in Φ_2) independently of the values of the mixing angles θ_{ij}^L. It will prove convenient to introduce a matrix

$$A \equiv \begin{pmatrix} 1 & -\frac{\widetilde{m}^\star_{\nu 12}}{\widetilde{m}^\star_{\nu 11}} & \frac{(\widetilde{m}_\nu^{-1})^\star_{13}}{(\widetilde{m}_\nu^{-1})^\star_{33}} \\ \frac{\widetilde{m}_{\nu 12}}{\widetilde{m}_{\nu 11}} & 1 & \frac{(\widetilde{m}_\nu^{-1})^\star_{23}}{(\widetilde{m}_\nu^{-1})^\star_{33}} \\ \frac{\widetilde{m}_{\nu 13}}{\widetilde{m}_{\nu 11}} & -\frac{(\widetilde{m}_\nu^{-1})_{23}}{(\widetilde{m}_\nu^{-1})_{33}} & 1 \end{pmatrix} D_\Phi\,, \tag{3.7}$$

such that the elements of U_R can be written in the form

$$U_{Rij} = \frac{\min[m_{Di}, m_{Dj}]}{\max[m_{Di}, m_{Dj}]}\, A_{ij}\,. \tag{3.8}$$

One can also derive an expression for the orthogonal matrix starting from its definition $\Omega = D_m^{-\frac{1}{2}}\, U^\dagger\, m_D\, D_M^{-\frac{1}{2}}$ [37] that, using eq. (3.1), becomes [38]

$$\Omega = D_m^{-\frac{1}{2}}\, U^\dagger\, V_L^\dagger\, D_{m_D}\, U_R\, D_M^{-\frac{1}{2}}\,. \tag{3.9}$$

In terms of matrix elements this can be written as

$$\Omega_{ij} \simeq \frac{1}{\sqrt{m_i\, M_j}} \sum_k m_{Dl}\, U^\star_{ki}\, V^\star_{L\,lk}\, U_{R\,kj}\,, \tag{3.10}$$

[9] As pointed out in [31], the validity of these results relies on hierarchical RH neutrino masses, $M_3 \gg M_2 \gg M_1$ and breaks down in the close vicinity of crossing level solutions found in [36] where either $|\widetilde{m}_{\nu 11}|$ or $|(\widetilde{m}_\nu^{-1})_{33}|$ or both vanish. However, as we will point out, when $|\widetilde{m}_{\nu 11}|$ or $|(\widetilde{m}_\nu^{-1})_{33}|$ vanish separately, corresponding to $M_1 \simeq M_2$ and $M_2 \simeq M_3$ respectively, successful leptogenesis is not attained, and the case when they both get very small, leading to a compact spectrum $M_1 \sim M_2 \sim M_3$, necessarily implies a huge fine-tuning in the seesaw formula since in this case the orthogonal matrix elements become huge, as we are going to show. For this reason a hierarchical spectrum condition is not restrictive at all. We will be back on this point.

JHEP10(2017)029

from which one finds[10]

$$\Omega \simeq \begin{pmatrix} \frac{(\widetilde{m}_\nu W^\star)_{11}}{\sqrt{-m_1\,\widetilde{m}_{\nu 11}}} & \sqrt{\frac{m_2\,m_3\,(\widetilde{m}_\nu^{-1})_{33}}{\widetilde{m}_{\nu 11}}}\left(W^\star_{21} - W^\star_{31}\,\frac{(\widetilde{m}_\nu^{-1})_{23}}{(\widetilde{m}_\nu^{-1})_{33}}\right) e^{i\,(\rho+\sigma+\rho_L+\sigma_L)} & \frac{W^\star_{31}}{\sqrt{m_1\,(\widetilde{m}_\nu^{-1})_{33}}} \\ \frac{(\widetilde{m}_\nu W^\star)_{12}}{\sqrt{-m_2\,\widetilde{m}_{\nu 11}}} & \sqrt{\frac{m_1\,m_3\,(\widetilde{m}_\nu^{-1})_{33}}{\widetilde{m}_{\nu 11}}}\left(W^\star_{22} - W^\star_{32}\,\frac{(\widetilde{m}_\nu^{-1})_{23}}{(\widetilde{m}_\nu^{-1})_{33}}\right) e^{i\,(\rho+\sigma+\rho_L+\sigma_L)} & \frac{W^\star_{32}}{\sqrt{m_2\,(\widetilde{m}_\nu^{-1})_{33}}} \\ \frac{(\widetilde{m}_\nu W^\star)_{13}}{\sqrt{-m_3\,\widetilde{m}_{\nu 11}}} & \sqrt{\frac{m_1\,m_2\,(\widetilde{m}_\nu^{-1})_{33}}{\widetilde{m}_{\nu 11}}}\left(W^\star_{23} - W^\star_{33}\,\frac{(\widetilde{m}_\nu^{-1})_{23}}{(\widetilde{m}_\nu^{-1})_{33}}\right) e^{i\,(\rho+\sigma+\rho_L+\sigma_L)} & \frac{W^\star_{33}}{\sqrt{m_3\,(\widetilde{m}_\nu^{-1})_{33}}} \end{pmatrix}, \tag{3.11}$$

where we defined $W \equiv V_L\,U$.

Let us now discuss the calculation of the asymmetry. Since in section 4 we will also be interested in those solutions satisfying, in addition to successful leptogenesis, also the strong thermal condition, we can write the final asymmetry as the sum of two terms,

$$N^{\rm f}_{B-L} = N^{\rm p,f}_{B-L} + N^{\rm lep,f}_{\rm B-L}\,. \tag{3.12}$$

The first term is the relic value of the pre-existing asymmetry, the second is the asymmetry generated from leptogenesis. This of course would translate into a baryon-to-photon number ratio also given by the sum of two contributions, $\eta^{\rm p}_B$ and $\eta^{\rm lep}_B$ respectively. The typical assumption is that the initial pre-existing asymmetry, after inflation and prior to leptogenesis, is negligible. We also consider the possibility that some external mechanism might have generated a large value of the *initial* pre-existing asymmetry, $N^{\rm p,i}_{B-L}$, between the end of inflation and the onset of leptogenesis, i.e. a value that would translate, in the absence of any wash-out, into a sizeable value of $\eta^{\rm p}_B$. The strong thermal leptogenesis condition requires that this initial value of the pre-existing asymmetry is efficiently washed out by RH neutrinos wash-out processes in a way that the final value of η_B is dominated by $\eta^{\rm lep}_B$.[11] The predicted value of the baryon-to-photon number ratio is then entirely explained by the contribution from leptogenesis,

$$\eta^{\rm lep}_B = a_{\rm sph}\,\frac{N^{\rm lep,f}_{B-L}}{N^{\rm rec}_\gamma} \simeq 0.96\times 10^{-2}\,N^{\rm lep,f}_{B-L}\,, \tag{3.13}$$

accounting for sphaleron conversion [40, 41] and photon dilution and where, in the last numerical expression, we normalised the abundances N_X of any generic quantity X in a way that the ultra-relativistic equilibrium abundance of a RH neutrino $N^{\rm eq}_{N_i}(T \gg M_i) = 1$. Successful leptogenesis requires that $\eta^{\rm lep}_B$ reproduces the experimental value that, from *Planck* data (including lensing) combined with external data sets [34], is given by

$$\eta^{\rm CMB}_B = (6.10 \pm 0.04)\times 10^{-10}\,. \tag{3.14}$$

For both two terms in eq. (3.12) we can give analytic expressions. The relic value of the pre-existing asymmetry has to be calculated [23, 30, 42] as $N^{\rm p,f}_{B-L} = \sum_\alpha N^{\rm p,f}_{\Delta_\alpha}$, with each

[10] This improves the analytical expression given in [39] where the approximation $W \simeq U$ was used. We checked that this analytic expression perfectly reproduces the numerical results. This expression shows explicitly how approaching the crossing level solutions, for vanishing $|\widetilde{m}_{\nu 11}|$ or $|(\widetilde{m}_\nu^{-1})_{33}|$, the $|\Omega^2_{ij}|$'s become huge and this corresponds to very fine-tuned cancellations in the seesaw formula.

[11] For definiteness we adopt a criterium $\eta^{\rm p}_B < 0.1\,\eta^{\rm lep}_B$ but in any case the constraints on low energy neutrino parameters depend only logarithmically on the precise maximum allowed value for $\eta^{\rm p}_B/\eta^{\rm lep}_B$.

JHEP10(2017)029

flavour contribution given by

$$N^{\rm p,f}_{\Delta_\tau} = \left(p^0_{{\rm p}\tau} + \Delta p_{{\rm p}\tau}\right) e^{-\frac{3\pi}{8}(K_{1\tau}+K_{2\tau})} N^{\rm p,i}_{B-L}, \tag{3.15}$$

$$N^{\rm p,f}_{\Delta_\mu} = \left\{\left(1-p^0_{{\rm p}\tau}\right)\left[p^0_{\mu\tau_2^\perp} p^0_{{\rm p}\tau_2^\perp} e^{-\frac{3\pi}{8}(K_{2e}+K_{2\mu})} + \left(1-p^0_{\mu\tau_2^\perp}\right)\left(1-p^0_{{\rm p}\tau_2^\perp}\right)\right] + \Delta p_{{\rm p}\mu}\right\} e^{-\frac{3\pi}{8}K_{1\mu}} N^{\rm p,i}_{B-L},$$

$$N^{\rm p,f}_{\Delta_e} = \left\{\left(1-p^0_{{\rm p}\tau}\right)\left[p^0_{e\tau_2^\perp} p^0_{{\rm p}\tau_2^\perp} e^{-\frac{3\pi}{8}(K_{2e}+K_{2\mu})} + \left(1-p^0_{e\tau_2^\perp}\right)\left(1-p^0_{{\rm p}\tau_2^\perp}\right)\right] + \Delta p_{{\rm p}e}\right\} e^{-\frac{3\pi}{8}K_{1e}} N^{\rm p,i}_{B-L}.$$

In this expression the $K_{i\alpha}$'s are the *flavoured decay parameters* defined by

$$K_{i\alpha} \equiv \frac{\Gamma_{i\alpha} + \overline{\Gamma}_{i\alpha}}{H\left(T = M_i\right)} = \frac{|m_{D\alpha i}|^2}{M_i\, m_\star}\,, \tag{3.16}$$

where $\Gamma_{i\alpha} = \Gamma(N_i \to \phi^\dagger\, l_\alpha)$ and $\bar{\Gamma}_{i\alpha} = \Gamma(N_i \to \phi\, \bar{l}_\alpha)$ are the zero temperature limit of the flavoured decay rates into α leptons and anti-leptons in the three-flavoured regime, $m_\star \simeq 1.1 \times 10^{-3}\,{\rm eV}$ is the equilibrium neutrino mass, $H(T) = \sqrt{g_\star^{SM}\, 8\,\pi^3/90}\, T^2/M_{\rm P}$ is the expansion rate and $g_\star^{SM} = 106.75$ is the SM number of ultra-relativistic degrees of freedom. Using the bi-unitary parameterisation eq. (3.1), the flavoured decay parameters can be written as

$$K_{i\alpha} = \frac{\sum_{k,l}\, m_{Dk}\, m_{Dl}\, V_{Lk\alpha}\, V^\star_{Ll\alpha}\, U^\star_{Rki}\, U_{Rli}}{M_i\, m_\star}\,. \tag{3.17}$$

The quantities $p^0_{{\rm p}\tau}$ and $p^0_{{\rm p}\tau_2^\perp}$ indicate the fractions of the pre-existing asymmetry in the tauon flavour and in the flavour $\tau_2^\perp$, the electron and muon flavours superposition component in the leptons produced by the N_2-decays (or equivalently the flavour component that is washed-out in the inverse processes producing N_2) so that $p^0_{{\rm p}\tau} + p^0_{{\rm p}\tau_2^\perp} = 1$. The two quantities $p^0_{\alpha\tau_2^\perp} \equiv K_{2\alpha}/(K_{2e} + K_{2\mu})$ $(\alpha = e, \mu)$ are then the fractions of α-asymmetry in the $\tau_2^\perp$ component, so that $p^0_{e\tau_2^\perp} + p^0_{\mu\tau_2^\perp} = 1$.

The contribution from leptogenesis also has to be calculated as the sum of three contributions from each flavour, explicitly

$$N^{\rm lep,f}_{B-L} = N^{\rm lep,f}_{\Delta_e} + N^{\rm lep,f}_{\Delta_\mu} + N^{\rm lep,f}_{\Delta_\tau}\,. \tag{3.18}$$

The expression we derived for M_1 from the SO(10) inspired conditions, the first of the eqs. (3.4), implies $M_1 \ll 10^9\,{\rm GeV}$ and in this case the asymmetry produced from N_1 decays is negligible [46, 47]. On the other hand M_2 can be sufficiently large[12] for the asymmetry produced from N_2-decays to reproduce the observed asymmetry: for this reason SO(10)-inspired conditions necessarily require a N_2-dominated scenario of leptogenesis.[13] Moreover since just marginal solutions are found for $M_2 \gtrsim 10^{12}\,{\rm GeV}$, where the production occurs in the unflavoured regime, one has to consider a two-flavour regime for the asymmetry production from N_2 decays. In this case the three flavoured asymmetries can be calculated

[12] A lower bound $M_2 \gtrsim 5 \times 10^{10}\,{\rm GeV}$ was found in [33].

[13] In principle one should also consider the asymmetry produced from N_3 decays occurring in the unflavoured regime since $M_3 \gg 10^{12}\,{\rm GeV}$. However the *CP* asymmetry ε_3 is suppressed as M_2/M_3 compared to ε_2 and in the end it turns out that also the contribution to the asymmetry from N_3 decays, as that one from N_1 decays, is negligible.

JHEP10(2017)029

using [16, 43–45][14]

$$N^{\rm lep,f}_{\Delta_e} \simeq \left[\frac{K_{2e}}{K_{2\tau_2^\perp}}\,\varepsilon_{2\tau_2^\perp}\,\kappa\left(K_{2\tau_2^\perp}\right) + \left(\varepsilon_{2e} - \frac{K_{2e}}{K_{2\tau_2^\perp}}\,\varepsilon_{2\tau_2^\perp}\right)\,\kappa\left(K_{2\tau_2^\perp}/2\right)\right]\, e^{-\frac{3\pi}{8}\,K_{1e}}\,,$$
$$N^{\rm lep,f}_{\Delta_\mu} \simeq \left[\frac{K_{2\mu}}{K_{2\tau_2^\perp}}\,\varepsilon_{2\tau_2^\perp}\,\kappa\left(K_{2\tau_2^\perp}\right) + \left(\varepsilon_{2\mu} - \frac{K_{2\mu}}{K_{2\tau_2^\perp}}\,\varepsilon_{2\tau_2^\perp}\right)\,\kappa\left(K_{2\tau_2^\perp}/2\right)\right]\, e^{-\frac{3\pi}{8}\,K_{1\mu}}\,,$$
$$N^{\rm lep,f}_{\Delta_\tau} \simeq \varepsilon_{2\tau}\,\kappa\left(K_{2\tau}\right)\, e^{-\frac{3\pi}{8}\,K_{1\tau}}\,, \tag{3.19}$$

where $\varepsilon_{2\alpha} \equiv -(\Gamma_{2\alpha} - \overline{\Gamma}_{2\alpha})/(\Gamma_2 + \overline{\Gamma}_2)$ are the N_2-flavoured CP asymmetries ($\alpha = e, \mu, \tau$), with $\Gamma_2 \equiv \sum_\alpha \Gamma_{2\alpha}$ and $\overline{\Gamma}_2 \equiv \sum_\alpha \overline{\Gamma}_{2\alpha}$, and simply $\varepsilon_{2\tau_2^\perp} \equiv \varepsilon_{2e} + \varepsilon_{2\mu}$ and $K_{2\tau_2^\perp} \equiv K_{2e} + K_{2\mu}$. For the efficiency factors at the production $\kappa(K_{2\alpha})$ we used the standard analytic expression [47]

$$\kappa(K_{2\alpha}) = \frac{2}{z_B(K_{2\alpha})\,K_{2\alpha}}\left(1 - e^{-\frac{K_{2\alpha}\,z_B(K_{2\alpha})}{2}}\right)\,,\quad z_B(K_{2\alpha}) \simeq 2 + 4\,K_{2\alpha}^{0.13}\,e^{-\frac{2.5}{K_{2\alpha}}}\,. \tag{3.20}$$

This expression holds for an initial thermal abundance but since all solutions we found are for strong wash-out at the production (either $K_{2\tau} \gg 1$ or $K_{2\tau_2^\perp} \gg 1$ respectively for tauon and muon-dominated solutions), the asymmetry does not depend on the initial N_2 abundance anyway. Moreover in the strong wash-out regime the theoretical uncertainties are within 20% [11–15, 48].[15]

The flavoured CP asymmetries can be calculated using [49]

$$\varepsilon_{2\alpha} \simeq \bar{\varepsilon}(M_2)\,\left\{\mathcal{I}_{23}^\alpha\,\xi(M_3^2/M_2^2) + \mathcal{J}_{23}^\alpha\,\frac{2}{3(1 - M_2^2/M_3^2)}\right\}\,, \tag{3.21}$$

where we introduced

$$\bar{\varepsilon}(M_2) \equiv \frac{3}{16\,\pi}\,\frac{M_2\,m_{\rm atm}}{v^2}\,,\qquad \xi(x) = \frac{2}{3}x\left[(1+x)\ln\left(\frac{1+x}{x}\right) - \frac{2-x}{1-x}\right]\,, \tag{3.22}$$

$$\mathcal{I}_{23}^\alpha \equiv \frac{{\rm Im}\left[m^\star_{D\alpha 2}m_{D\alpha 3}(m_D^\dagger\,m_D)_{23}\right]}{M_2\,M_3\,\widetilde{m}_2\,m_{\rm atm}}\ \text{ and }\ \mathcal{J}_{23}^\alpha \equiv \frac{{\rm Im}\left[m^\star_{D\alpha 2}\,m_{D\alpha 3}(m_D^\dagger\,m_D)_{32}\right]}{M_2\,M_3\,\widetilde{m}_2\,m_{\rm atm}}\,\frac{M_2}{M_3}, \tag{3.23}$$

[14] These equations for the calculation of the final asymmetry hold for $100\,{\rm GeV} \lesssim M_1 \lesssim 10^9\,{\rm GeV}$, in the N_2-dominated scenario. While the upper bound is basically always valid within given SO(10)-inspired conditions, except for a very fine-tuned case corresponding to very small value of $\widetilde{m}_{\nu 11}$ (we will be back on this case), the lower bound in principle could be violated if $\alpha_1 \lesssim 0.1$. In this case there is no wash-out from the lightest RH neutrino and the exponentials would disappear and consequently all constraints on low energy neutrino parameters. This scenario has been discussed in [32].

[15] Notice that since the constraints on the low energy neutrino parameters are determined mainly by the vanishing of the $K_{1\alpha}$ in the exponentials, these depend only logarithmically on the asymmetry and a theoretical uncertainty of 20% on the asymmetry translates into a less than 1% theoretical uncertainty on the constraints. In any case improvements in this direction will also be needed in future.

JHEP10(2017)029

with $\widetilde{m}_2 \equiv (m_D^\dagger\, m_D)_{22}/M_2$. Since $M_3 \gg M_2$, one can approximate $\xi(M_3^2/M_2^2) \simeq 1$ and neglect the second term $\propto \mathcal{J}_{23}^\alpha$ in the eq. (3.21).[16] Using the singular value decomposition eq. (3.1) for m_D, one obtains

$$\varepsilon_{2\alpha} \simeq \frac{3}{16\,\pi\,v^2}\,\frac{|(\widetilde{m}_\nu)_{11}|}{m_1\,m_2\,m_3}\,\frac{\sum_{k,l}\,m_{Dk}\,m_{Dl}\,\mathrm{Im}[V_{Lk\alpha}\,V^\star_{Ll\alpha}\,U^\star_{Rk2}\,U_{Rl3}\,U^\star_{R32}\,U_{R33}]}{|(\widetilde{m}_\nu^{-1})_{33}|^2+|(\widetilde{m}_\nu^{-1})_{23}|^2}\,, \tag{3.24}$$

where in $(m_D^\dagger\, m_D)_{22} = \sum_k\, m_{Dk}^2\,|U_{Rk2}|^2$ we neglected the term $k=1$, suppressed as $(m_{D1}/m_{D2})^2$ compared to the others, and we have also approximated $(m_D^\dagger\, m_D)_{23} \simeq m_{D3}^2\,U^\star_{R32}\,U_{R33}$.

Except for special points where $\varepsilon_{2e} \simeq \varepsilon_{2\mu}$, one of the two (typically $\varepsilon_{2\mu}$) dominates on the other and this implies that the terms in $N^{\mathrm{lep,f}}_{\Delta_e}$ and $N^{\mathrm{lep,f}}_{\Delta_\mu}$ in round brackets, the so called phantom terms [44, 45], are necessarily negligible and one obtains much simpler expressions,[17]

$$\begin{aligned}
N^{\mathrm{lep,f}}_{\Delta_e} &\simeq \varepsilon_{2e}\,\kappa(K_{2e}+K_{2\mu})\,e^{-\frac{3\pi}{8}K_{1e}}\,,\\
N^{\mathrm{lep,f}}_{\Delta_\mu} &\simeq \varepsilon_{2\mu}\,\kappa(K_{2e}+K_{2\mu})\,e^{-\frac{3\pi}{8}K_{1\mu}}\,,\\
N^{\mathrm{lep,f}}_{\Delta_\tau} &\simeq \varepsilon_{2\tau}\,\kappa(K_{2\tau})\,e^{-\frac{3\pi}{8}K_{1\tau}}\,,
\end{aligned} \tag{3.25}$$

where we wrote again $N^{\mathrm{lep,f}}_{\Delta_\tau}$ for completeness. In this way, using the analytic expression eq. (3.5) for U_R, eq. (3.24) for the $\varepsilon_{2\alpha}$'s and eq. (3.17) for the $K_{i\alpha}$'s, and given an expression for V_L, one obtains a full analytical expression for the asymmetry depending on the low energy neutrino parameters, on V_L and on the α_i's.[18] In the appendix we summarise all this set of analytic expressions that basically constitute the analytical solution we found.

If one adopts the approximation $V_L = I$, from the eq. (3.24) one obtains for the $\varepsilon_{2\alpha}$'s [31]

$$\varepsilon_{2\alpha} \simeq \frac{3\,m_{D\alpha}^2}{16\,\pi\,v^2}\,\frac{m_{ee}}{m_1\,m_2\,m_3}\,\frac{\mathrm{Im}[U^\star_{R\alpha2}\,U_{R\alpha3}\,U^\star_{R32}\,U_{R33}]}{|(m_\nu^{-1})_{\tau\tau}|^2+|(m_\nu^{-1})_{\mu\tau}|^2}\,. \tag{3.26}$$

From this one it is then easy to obtain explicitly

$$\begin{aligned}
\varepsilon_{2\tau} &\simeq \frac{3\,m_{D2}^2}{16\,\pi\,v^2}\,\frac{m_{ee}\,\left[|(m_\nu^{-1})_{\tau\tau}|^2+|(m_\nu^{-1})_{\mu\tau}|^2\right]^{-1}}{m_1\,m_2\,m_3}\,\frac{|(m_\nu^{-1})_{\mu\tau}|^2}{|(m_\nu^{-1})_{\tau\tau}|^2}\,\sin\alpha_L\,, \qquad (3.27)\\
\varepsilon_{2\mu} &\simeq -\frac{m_{D2}^2}{m_{D3}^2}\,\varepsilon_{2\tau}\,,\\
\varepsilon_{2e} &\simeq \frac{3\,m_{D1}^2}{16\,\pi\,v^2}\,\frac{m_{D1}^2}{m_{D3}^2}\,\frac{|m_{\nu e\mu}|\,\left[|(m_\nu^{-1})_{\tau\tau}|^2+|(m_\nu^{-1})_{\mu\tau}|^2\right]^{-2}}{m_1\,m_2\,m_3}\,\frac{|(m_\nu^{-1})_{e\tau}|\,|(m_\nu^{-1})_{\mu\tau}|}{|(m_\nu^{-1})_{\tau\tau}|^2}\,\sin\alpha_L^e\,,
\end{aligned}$$

[16] This hierarchical approximation has been tested since we used the exact expression for ξ, able to describe a resonant enhancement, and we did not neglect the term $\mathcal{J}_{23}^\alpha$ in the numerical results and we checked that no new quasi-degenerate solutions are found for $M_1 \lesssim 10^9$ GeV (i.e. within the N_2-dominated scenario) [23]. We will come back on this point when we will discuss theoretical uncertainties at the end of this section.

[17] Like for the hierarchical approximation, we indeed also checked that phantom terms, that are kept in numerical results, do not play any role and can be neglected in SO(10)-inspired leptogenesis.

[18] Notice however that the dependence on α_1 and on α_3 cancels out in physical solutions satisfying successful leptogenesis [31, 33]).

JHEP10(2017)029

implying

$$\varepsilon_{2\tau}^{\max} : \varepsilon_{2\mu}^{\max} : \varepsilon_{2e}^{\max} \sim 1 : \frac{m_{D2}^2}{m_{D3}^2} : \frac{m_{D2}^2}{m_{D3}^2}\,\frac{m_{D1}^4}{m_{D2}^4}\,, \tag{3.28}$$

where we maximised over the phase factors given by

$$\alpha_L = \mathrm{Arg}\,[m_{\nu ee}] - 2\,\mathrm{Arg}[(m_\nu^{-1})_{\mu\tau}] - \pi - 2\,(\rho+\sigma)\,, \tag{3.29}$$

and

$$\alpha_L^e = \mathrm{Arg}\,[m_{\nu e\mu}] - \mathrm{Arg}[(m_\nu^{-1})_{\mu\tau}] - \mathrm{Arg}[(m_\nu^{-1})_{e\tau}] - \pi - 2\,(\rho+\sigma)\,. \tag{3.30}$$

The electron *CP* asymmetry is so strongly suppressed (more than fifteen orders of magnitude compared to the tauonic) that the corresponding contribution to the final asymmetry is completely negligible. The muon *CP* asymmetry is also suppressed compared to the tauonic *CP* asymmetry by about four orders of magnitude but it might be still large enough to allow the existence of (marginal) muon-dominated solutions. However, when the washout both at the production and from the lightest RH neutrino is also taken into account, one finds that also the muon contribution to the final asymmetry is always much below the observed value and one does not find any muon-dominated solution for $V_L = I$ [33]. Therefore, the electron and muon contributions are never able to reproduce the observed asymmetry and the final asymmetry can be approximated just by the tauon contribution, so that we can write [31, 32]

$$\begin{aligned} N_{B-L}^{\mathrm{lep,f}}\Big|_{V_L=I} \simeq \frac{3}{16\,\pi}\,\frac{m_{D2}^2}{v^2}\,\frac{|m_{\nu ee}|\,(|m_{\nu\tau\tau}^{-1}|^2 + |m_{\nu\mu\tau}^{-1}|^2)^{-1}}{m_1\,m_2\,m_3}\,\frac{|m_{\nu\mu\tau}^{-1}|^2}{|m_{\nu\tau\tau}^{-1}|^2}\,\sin\alpha_L \\ \times\,\kappa\left(\frac{m_1\,m_2\,m_3}{m_\star}\,\frac{|(m_\nu^{-1})_{\mu\tau}|^2}{|m_{\nu ee}|\,|(m_\nu^{-1})_{\tau\tau}|}\right) \\ \times\, e^{-\frac{3\pi}{8}\,\frac{|m_{\nu e\tau}|^2}{m_\star\,|m_{\nu ee}|}}\,, \end{aligned} \tag{3.31}$$

where for the $K_{i\alpha}$'s we used [31]

$$K_{i\alpha} = \frac{m_{D\alpha}^2}{M_i\,m_\star}\,|U_{R\alpha i}|^2\,, \tag{3.32}$$

that can be easily derived from the eq. (3.17) for $V_L = I$, obtaining

$$K_{1\tau} \simeq \frac{m_{D3}^2}{m_\star\,M_1}\,|U_{R31}|^2 \simeq \frac{|m_{\nu e\tau}|^2}{m_\star\,|m_{\nu ee}|} \tag{3.33}$$

and

$$K_{2\tau} \simeq \frac{m_{D3}^2}{m_\star\,M_2}\,|U_{R32}|^2 \simeq \frac{m_1\,m_2\,m_3}{m_\star}\,\frac{|(m_\nu^{-1})_{\mu\tau}|^2}{|m_{\nu ee}|\,|(m_\nu^{-1})_{\tau\tau}|}\,. \tag{3.34}$$

In figure 1 we show scatter plots of solutions for successful SO(10)-inspired leptogenesis in the seesaw parameter space projected on planes for different choices of two low energy neutrino parameters. We distinguish in yellow and orange the tauon-dominated solutions, corresponding respectively to $I \leq V_L \leq V_{\mathrm{CKM}}$ and $V_L = I$, and in green the muon-dominated solutions realised only for $I \leq V_L \leq V_{\mathrm{CKM}}$. The variation of the low energy

JHEP10(2017)029

neutrino parameters is within the indicated ranges.[19] The plots have been obtained for $(\alpha_1, \alpha_2, \alpha_3) = (1, 5, 1)$. We have also used[20] $(m_{\rm u}, m_{\rm c}, m_{\rm t}) = (1\,{\rm MeV}, 400\,{\rm MeV}, 100\,{\rm GeV})$ for the values of the up quark masses at the leptogenesis scale $T_L \simeq (3\text{–}10)\,10^{10}\,{\rm GeV}$ [50].

We also show the subset of solutions satisfying in addition the strong thermal condition (light blu for $I \leq V_L \leq V_{\rm CKM}$ and dark blue for $V_L = I$) for an initial pre-existing asymmetry $N^{\rm p,i}_{B-L} = 10^{-3}$. The scatter plots have been obtained for an initial thermal N_2 abundance but, as we will discuss, the solutions do not depend on the initial value of N_{N_2}. We have also imposed $M_\Omega \equiv \max_{i,j}[|\Omega^2_{ij}|] = 100$. With these conditions we haven't found any electronic-dominated solution, even for $I \leq V_L \leq V_{\rm CKM}$, we will be back on this point. Contrarily to α_1 and α_3 that cancel out in the final asymmetry, the parameter $\alpha_2 \equiv m_{D2}/m_{\rm c}$ plays clearly a very important role since all N_2 *CP* asymmetries are proportional to the square of this parameter. We have set $\alpha_2 = 5$ as maximum reference value. The dependence of the constraints on α_2 was studied in detail in [33] where the lower bound $\alpha_2 \gtrsim 1$ was found. There is no of course upper bound from leptogenesis but in realistic models this is never found too much larger than our reference value $\alpha_2 = 5$. For example it is interesting that in the realistic fits found in [51] within SO(10) models one has $\alpha_2 \lesssim 6$, very close to our reference maximum value.

Before concluding this section we want to comment on the approximations of our results that might give rise to some corrections that should be therefore considered sources of theoretical uncertainties in our calculation.

- We are using Boltzmann equations and for this reason we have imposed $M_2 \lesssim 10^{12}\,{\rm GeV}$, where a two-flavour regime is realised at the N_2 production and Boltzmann equations can be used. If $M_2 \gg 10^{12}\,{\rm GeV}$ the production would occur in the unflavoured regime and the wash-out at production would be much higher and indeed if one also calculates the asymmetry in this regime one finds very marginal points as discussed in detail in [23]. One could therefore wonder whether in a density matrix approach, describing the transition between the two regimes, one could find a suppression of solutions already between $10^{11}\,{\rm GeV}$ and $10^{12}\,{\rm GeV}$. However, we should say that for $\alpha_2 < 5$ and $M_\Omega < 100$, as we are setting, in any case one does not find M_2 to be much larger than $10^{11}\,{\rm GeV}$. Therefore, we do not expect much more stringent constraints from a density matrix formalism for $\alpha_2 \lesssim 5$.

- We are using a hierarchical approximation $M_3 \gtrsim M_2$. However checks in [23] have found new quasi-degenerate solutions only at very large m_1 values, $m_1 \gtrsim 1\,{\rm eV}$, anyway cosmologically excluded. We are neglecting just the case of a compact spectrum $M_1 \sim M_2 \sim M_3 \sim 10^{10}\,{\rm GeV}$ realised when both $|\widetilde{m}_{\nu 11}|$ and $|(\widetilde{m}^{-1}_\nu)_{33}|$ get

[19] To be conservative we used 4σ intervals in eq. (2.5) and δ is allowed to vary in the whole range $[-\pi, \pi]$.

[20] Since the final asymmetry $\propto m^2_{D2} = (\alpha_2\, m_{\rm c})^2$, for a given value of α_2, the theoretical uncertainty in the determination of the value of $m_{\rm c}$ at the leptogenesis scale translates into a (doubled) theoretical uncertainty in the determination of the final asymmetry: the value of the charm quark mass at the scale of leptogenesis is then one of the most important sources of uncertainties.

JHEP10(2017)029

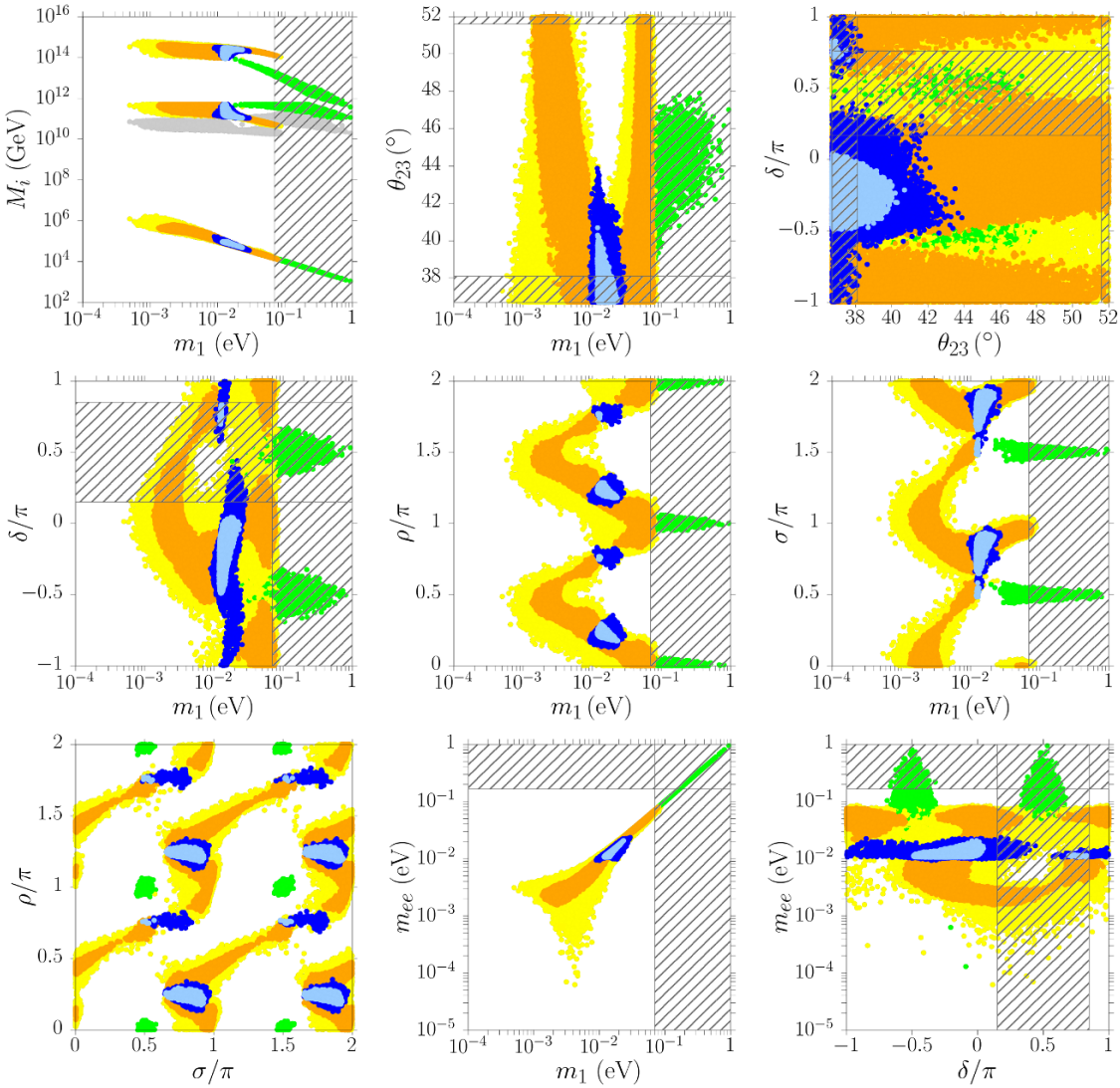

Figure 1. Scatter plots in the seesaw parameter space projected on different planes for NO and $(\alpha_1, \alpha_2, \alpha_3 = 1, 5, 1)$. All points satisfy (at $\simeq 3\sigma$) successful leptogenesis. The yellow points correspond to tauon-dominated solutions for an initial vanishing pre-existing asymmetry (light yellow for $I \leq V_L \leq V_{\rm CKM}$ and orange for $V_L = I$) The blue points are the subset satisfying the additional strong thermal condition for an initial value of the pre-existing asymmetry $N^{\rm p,i}_{B-L} = 10^{-3}$ (dark blue for $I \leq V_L \leq V_{\rm CKM}$ and light blue for $V_L = I$). The green points correspond to muon-dominated solutions. The solutions have been obtained for $M_\Omega = 100$ and imposing $M_3 > 2\, M_2$. The dashed bands indicate the 3σ excluded ranges for the corresponding mixing parameters (see eq. (2.5)), while for m_1 and m_{ee} they indicate the 95%C.L. and 90%C.L. upper bounds from *Planck* and KamLAND-Zen.

JHEP10(2017)029

sufficiently small.[21] The conditions for this compact spectrum were studied in [36] and more recently, including flavour effects and within a realistic model, in [52]. However, as already noticed in [31], this special case necessarily implies a huge fine-tuning in the seesaw formula.[22] In any case a compact spectrum solution gives rise to a distinct set of constraints on low energy neutrino parameters [52], in particular it predicts no signal in $0\nu\beta\beta$ experiments since $m_{ee} \lesssim 1\,\text{meV}$, while in our case the bulk of the solutions implies a detectable signal despite NO.

- We are neglecting the running of the parameters (including a precise evaluation of the charm quark mass at the scale of leptogenesis). This is not expected to be able to change significantly our results but of course in a not too far future, with an increase of the experimental precision on θ_{23} and δ it might become necessary to include the running from radiative corrections.

- Another approximation we are using, and that might be a source of theoretical uncertainties, is that we are neglecting flavour coupling [44]. This generates new terms in the asymmetry (though usually sub-dominant) that can open new solutions and relax the constraints. An example was found in [39], though the solution was also requiring some large amount of fine tuning in the seesaw formula. On the basis of preliminary results, we can say that flavour coupling introduces only corrections to the analytical expression we found or it adds solutions involving great amount of fine-tuning in the see-saw formula [53].

Our analytic solution will be actually very useful for a future derivation of the constraints including these effects, since it provides a new tool to generate solutions in a much faster way and likely also to understand analytically the impact of the various effects.

4 Decrypting the impact of $V_L \simeq V_{\text{CKM}}$

In this section we want to understand the impact of turning on $V_L \simeq V_{\text{CKM}}$ using the analytical expressions obtained in the previous section. Since V_L is unitary, this can be parameterised analogously to the leptonic mixing matrix as

$$V_L = \begin{pmatrix} c^L_{12}\,c^L_{13} & s^L_{12}\,c^L_{13} & s^L_{13}\,e^{-\mathrm{i}\delta_L} \\ -s^L_{12}\,c^L_{23} - c^L_{12}\,s^L_{23}\,s^L_{13}\,e^{\mathrm{i}\delta_L} & c^L_{12}\,c^L_{23} - s^L_{12}\,s^L_{23}\,s^L_{13}\,e^{\mathrm{i}\delta_L} & s^L_{23}\,c^L_{13} \\ s^L_{12}\,s^L_{23} - c^L_{12}\,c^L_{23}\,s^L_{13}\,e^{\mathrm{i}\delta_L} & -c^L_{12}\,s^L_{23} - s^L_{12}\,c^L_{23}\,s^L_{13}\,e^{\mathrm{i}\delta_L} & c^L_{23}\,c^L_{13} \end{pmatrix} \text{diag}\left(e^{i\rho_L}, 1, e^{i\sigma_L}\right), \tag{4.1}$$

[21] The reason why solutions in the vicinity of the crossing level $M_2 \sim M_3 \sim 10^{13}\,\text{GeV}$, realised when only $|(\widetilde{m}_\nu^{-1})_{33}|$ tends to vanish is that in this case $K_{2\tau} \propto |(\widetilde{m}_\nu^{-1})_{33}|^{-1}$ tends to become huge and together with it of course K_2 so that at the production one has a very strong wash-out and even the resonant enhancement of the CP asymmetries does not help. Of course in addition in any case one would also have huge fine-tuning in the seesaw formula. The crossing level for which $M_1 \sim M_2 \sim 10^7\,\text{GeV}$ when $|\widetilde{m}_{\nu 11}|$ vanish is also excluded since in this case, even worse, $K_{1\tau} \propto |\widetilde{m}_{\nu 11}|^{-1}$. For this reason only a compact spectrum is left as a (very fine-tuned) caveat to a hierarchical spectrum.

[22] It should be clear that the fine tuning is not only at the level of choosing the correct value of the degeneracy to realise the right asymmetry, but also more seriously, as already noticed in the footnote 8, from a comparison of the expressions eq. (3.4) with eq. (3.11) for Ω, at the level of the seesaw formula.

JHEP10(2017)029

having introduced three mixing angles $\theta_{12}^L, \theta_{13}^L$ and θ_{23}^L ($s_{ij}^L \equiv \sin\theta_{ij}^L$ and $c_{ij} \equiv \cos\theta_{ij}^L$), one Dirac-like phase δ_L and two Majorana-like phases ρ_L and σ_L. We want to understand analytically the effects of non-vanishing θ_{ij}^L with values at the level of the respective angles in $V_{\rm CKM}$ (see footnote 1), effects that have been so far found only numerically.

As we said, we will focus on NO, since for IO the allowed regions, in the non-supersymmetric framework we are considering and for $\alpha_2 \lesssim 5$, are marginal (in particular they require necessarily θ_{23} in the second octant and $m_1 \gtrsim 10\,\text{meV}$ implying $\sum_i m_i \gtrsim 0.11\,\text{eV}$, slightly disfavoured by current cosmological observations) and they completely disappear in the case of strong thermal leptogenesis.[23] These effects can be summarised as follows:

- Turning on $V_L \simeq V_{\rm CKM}$ enlarges the allowed region for tauon-dominated solutions relaxing the constraint on the low energy neutrino parameters. There are two interesting features that should be understood with an analytic description:

  (i) Within tauon-dominated solutions, there is a subset of solutions satisfying also the strong thermal condition [23, 31]. As one can see from the blue regions in the top central panel in figure 1, this subset is characterised by an upper bound on θ_{23} that for $V_L = I$ is given by $\theta_{23} \lesssim 41^\circ$ and for $I \leq V_L \lesssim V_{\rm CKM}$ relaxes to $\theta_{23} \lesssim 44^\circ$. The allowed range for δ also enlarges for a given value of θ_{23}. In the light of the current best fit value for $\theta_{23} \simeq 41^\circ$ (see eq. (2.5)), this is an interesting effect of turning on $V_L \simeq V_{\rm CKM}$ to be understood.

  (ii) the lower bound $m_{ee} \gtrsim 10^{-3}\,\text{eV}$ strongly relaxes to $m_{ee} \gtrsim 5 \times 10^{-5}\,\text{eV}$.

- While for $V_L = I$ there are only tauon-dominated solutions able to reproduce the observed asymmetry [38], muon-dominated solutions appear for $V_L \simeq V_{\rm CKM}$ and $0.01\,\text{eV} \lesssim m_1 \lesssim 1\,\text{eV}$ [23, 33], the largest possible m_1 values in SO(10)-inspired leptogenesis since tauon-dominated solutions are realised for $m_1 \lesssim 0.07\,\text{eV}$ (just at the edge of highest values allowed by cosmological observations). Thus they open a new region in low energy neutrino parameter space though currently disfavoured by the cosmological observations. We have not found electron-dominated solutions as in the supersymmetric framework [32, 54].

These are the main effects induced by $V_L \simeq V_{\rm CKM}$ that we want to understand analytically unpacking the solution we found.

4.1 *CP* asymmetries flavour ratio

We have seen that for $V_L = I$ the eq. (3.28) immediately shows how in this approximation one cannot reproduce electron and muon-dominated solutions. This result changes turning

[23] In the supersymmetric case, for large $\tan\beta \gtrsim 15$, one can have solutions for successful strong thermal leptogenesis even for IO [32].

JHEP10(2017)029

on $V_L \simeq V_{\rm CKM}$. We can use these two approximations in the eq. (3.24)

$$m^\star_{D\alpha 2} = \sum_k V_{Lk\alpha}\, m_{Dk}\, U^\star_{Rk2} \simeq m_{D2}\, (V_{L2\alpha}\, U^\star_{R22} + V_{L3\alpha}\, A^\star_{32})\,, \tag{4.2}$$
$$m_{D\alpha 3} = \sum_l V_{Ll\alpha}\, m_{Dl}\, U_{Rl3} \simeq m_{D3}\, V^\star_{L3\alpha}\, U_{R33}\,.$$

Notice that they give $\varepsilon_{2e} = \varepsilon_{2\mu} \simeq 0$ for $V_L = I$, something acceptable if one wants just to describe solutions giving successful leptogenesis since as we have seen, for $V_L = I$, there are not electron and muon-dominated solutions since the *CP* asymmetries are too small.

Using these approximations, from the eq. (3.24) one obtains for the three *CP* flavour asymmetries

$$\varepsilon_{2e} \simeq \frac{3\, m^2_{D2}}{16\,\pi\, v^2}\, \frac{|(\widetilde{m}_\nu)_{11}|}{m_1\, m_2\, m_3}\, \frac{{\rm Im}[V_{L12}\, V^\star_{L13}\, U^2_{R33}\, (A^\star_{32})^2]}{|(\widetilde{m}^{-1}_\nu)_{33}|^2 + |(\widetilde{m}^{-1}_\nu)_{23}|^2}\,, \tag{4.3}$$
$$\varepsilon_{2\mu} \simeq \frac{3\, m^2_{D2}}{16\,\pi\, v^2}\, \frac{|(\widetilde{m}_\nu)_{11}|}{m_1\, m_2\, m_3}\, \frac{{\rm Im}[V_{L22}\, V^\star_{L23}\, U^\star_{R22}\, U^2_{R33}\, A^\star_{32}]}{|(\widetilde{m}^{-1}_\nu)_{33}|^2 + |(\widetilde{m}^{-1}_\nu)_{23}|^2}\,, \tag{4.4}$$
$$\varepsilon_{2\tau} \simeq \frac{3\, m^2_{D2}}{16\,\pi\, v^2}\, \frac{|(\widetilde{m}_\nu)_{11}|}{m_1\, m_2\, m_3}\, \frac{|V_{L33}|^2\, {\rm Im}[U^2_{R33}\, (A^\star_{32})^2]}{|(\widetilde{m}^{-1}_\nu)_{33}|^2 + |(\widetilde{m}^{-1}_\nu)_{23}|^2}\,,$$

implying

$$\varepsilon^{\rm max}_{2\tau} : \varepsilon^{\rm max}_{2\mu} : \varepsilon^{\rm max}_{2e} \simeq 1 : |V_{L23}| : |V_{L21}\, V_{L31}|\,, \tag{4.5}$$

showing that this time, turning on the mixing angles in V_L, the tauon-dominated solutions are still favoured but potentially one can also have muon and even electron-dominated solutions.[24]

4.2 Tauon-dominated solutions and strong thermal leptogenesis

Let us start from the tauon flavour contribution. As already pointed out, for $V_L = I$ this is the only contribution that can reproduce the observed asymmetry [38] and, therefore, one has the simplified result $N^{\rm lep,f}_{B-L}\big|_{V_L=I} \simeq N^{\rm lep,f}_{\Delta_\tau}$. A full analytic description was given in [31], we already reviewed the analytic expressions for $\varepsilon_{2\tau}$ (eq. (3.27)), for the flavour decay parameters $K_{1\tau}$, $K_{2\tau}$ (see eqs. (3.33) and (3.34)) and for the final asymmetry (eq. (3.31)).

In the left panels figure 2 we are plotting the behaviour of all these quantities for a specific choice of the low energy neutrino parameters: we adopted the best fit values for θ_{12} and θ_{13} and then $\theta_{23} = 42°$, $\delta = -0.6\,\pi$. As one can see from the scatter plot in figure 1 in the plane δ versus θ_{23}, for this choice of values the observed asymmetry cannot be reproduced for $V_L = I$ (light blue points) since θ_{23} is too large. The plots in the bottom left panel of figure 2 confirm the result of the scatter plots. In the panels the thin black lines are the analytic expressions and one can see that they perfectly reproduce all numerical results.

[24] Notice also that turning on $V_L \neq I$ does not change the result that dominantly the $\varepsilon_{2\alpha} \propto m^2_{D2} = \alpha^2_2\, {m_{\rm c}}^2$ while they do not depend on α_1 and α_3.

JHEP10(2017)029

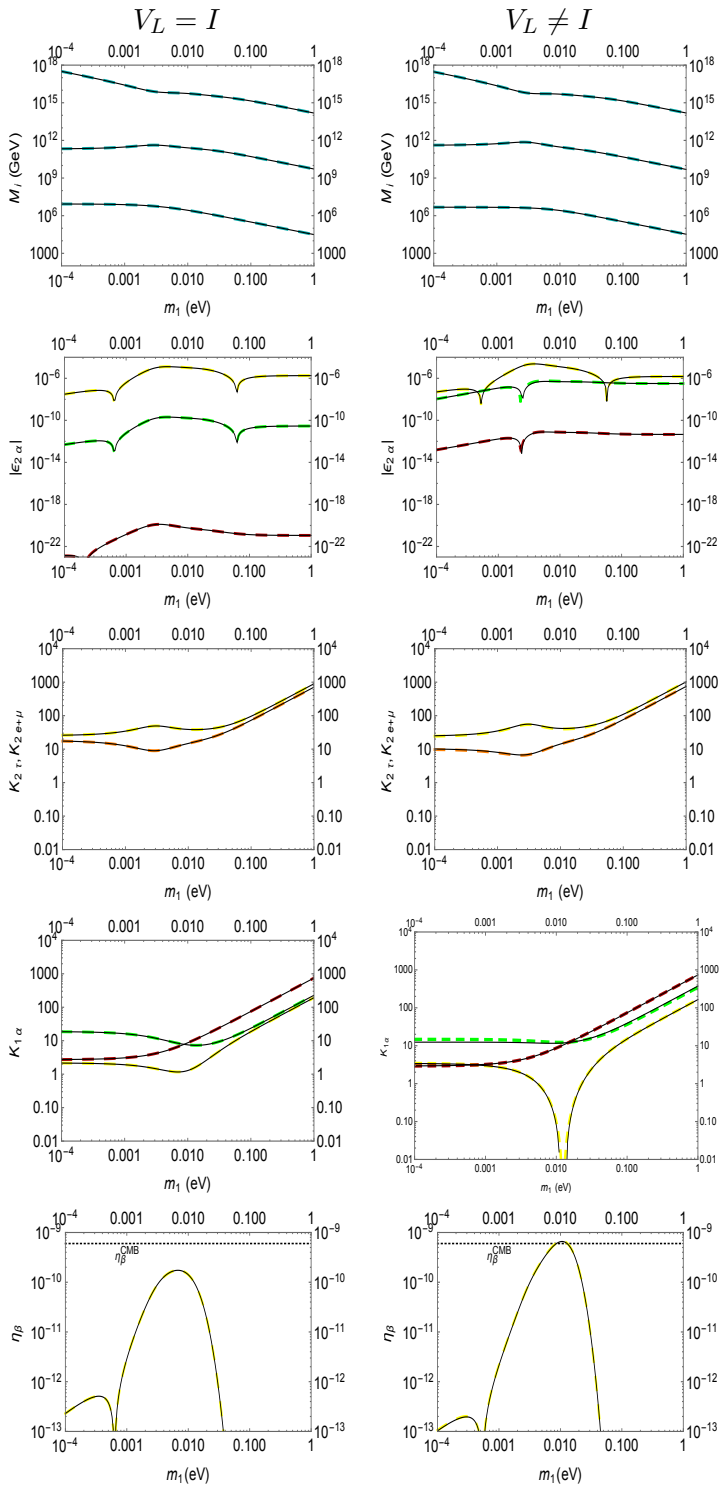

Figure 2. Example of (tauon-dominated) strong thermal solution. *Left panels*: $V_L = I$, $(\alpha_1, \alpha_2, \alpha_3) = (5, 5, 5)$, $(\theta_{13}, \theta_{12}, \theta_{23}) = (8.4°, 33°, 42°)$, $(\delta, \rho, \sigma) = (-0.6\pi, 0.23\pi, 0.78\,\pi)$; *Right panels*: same as for left panels but $V_L \neq I$ and $(\theta^L_{13}, \theta^L_{12}, \theta^L_{23}) = (0.1°, 9.5°, 2.4°)$ and $(\delta_L, \rho_L, \sigma_L) = (1.2\pi, 0.02\pi, 1.15\,\pi)$. All thin black lines are the analytical expressions for each corresponding quantity. The long-dashed coloured lines indicate the numerical results (same colour code as in figure 1: yellow for tauon flavour, green for muon flavour and red for electron flavour, the orange lines refer to the e+μ flavour).

JHEP10(2017)029

For $V_L \simeq V_{\rm CKM}$ all the expressions get generalised in the way we have seen. Let us specialise them and make more explicit for the tauon-dominated case. First of all for the tauonic *CP* asymmetry, considering only the dominant terms in the eq. (3.24) we find

$$\varepsilon_{2\tau} \simeq \frac{3m_{D2}^2}{16\pi v^2}\frac{|(\widetilde{m}_\nu)_{11}|}{m_1 m_2 m_3}\frac{|(\widetilde{m}_\nu^{-1})_{23}|}{|(\widetilde{m}_\nu^{-1})_{33}|}\frac{[|V_{L33}|^2(|(\widetilde{m}_\nu^{-1})_{23}|/|(\widetilde{m}_\nu^{-1})_{33}|)\sin\alpha_L^{\tau A}+|V_{L33}||V_{L23}|\sin\alpha_L^{\tau B}]}{|(\widetilde{m}_\nu^{-1})_{33}|^2+|(\widetilde{m}_\nu^{-1})_{23}|^2}, \tag{4.6}$$

where

$$\alpha_L^{\tau A} = \mathrm{Arg}\,[\widetilde{m}_{\nu 11}] - \mathrm{Arg}[(\widetilde{m}_\nu^{-1})_{23}] - \mathrm{Arg}[(\widetilde{m}_\nu^{-1})_{33}] - 2\,(\rho+\sigma) - 2\,(\rho_L+\sigma_L)\,, \tag{4.7}$$

$$\alpha_L^{\tau B} = \mathrm{Arg}\,[\widetilde{m}_{\nu 11}] - 2\,\mathrm{Arg}[(\widetilde{m}_\nu^{-1})_{23}] - \pi - 2\,(\rho+\sigma) - 2\,(\rho_L+\sigma_L)\,, \tag{4.8}$$

that generalises the eq. (4.4) for $V_L \neq I$. Notice that the second term is subdominant but still gives an important correction if θ_{23}^L is not too small. This analytic expression produced the black thin line in the second right panel in figure 2 and one can see that it perfectly fits the numerical result.

For the flavour decay parameters $K_{1\tau}$ and $K_{2\tau}$ we find respectively

$$K_{1\tau} \simeq \frac{1}{m_\star}\left(\frac{|\widetilde{m}_{\nu 13}|^2}{|\widetilde{m}_{\nu 11}|}|V_{L33}|^2 + 2\,\frac{V_{L23}\,V_{L33}^\star}{|\widetilde{m}_{\nu 11}|}\,\mathrm{Re}\,[\widetilde{m}_{\nu 12}^\star\,\widetilde{m}_{\nu 13}] + |V_{L23}|^2\,\frac{|\widetilde{m}_{\nu 13}|^2}{|\widetilde{m}_{\nu 11}|}\right) \tag{4.9}$$

and

$$K_{2\tau} \simeq \frac{m_1\,m_2\,m_3}{m_\star}\,\frac{|(\widetilde{m}_\nu^{-1})_{23}|^2}{|\widetilde{m}_{\nu 11}|\,|(\widetilde{m}_\nu^{-1})_{33}|}\,. \tag{4.10}$$

These analytic expressions also very well agree with the numerical results as it can be seen in the example of figure 2 in the right panels. In the case of $K_{1\tau}$ one needs more accuracy than for $K_{2\tau}$ since it suppresses exponentially the asymmetry and one needs to add also terms $\propto V_{L23}$ in order to get correctly the tauonic contribution to η_B, as one can see in the last right panel of figure 2 where the analytic contribution (thin black line) nicely matches the numerical results (yellow dashed line). There one can notice how the final asymmetry gets enhanced[25] by almost two orders of magnitude compared to the case $V_L = I$ and the main reason is that turning on $V_L \simeq V_{\rm CKM}$ makes now possible to have $K_{1\tau} \ll 1$ at larger values of θ_{23} and smaller values of δ something quite important considering that long baseline experiments such as NOνA and T2K are right now testing these parameters and in particular the deviation of θ_{23} from maximal mixing.

It is quite straightforward to extend the derivation of the upper bound on θ_{23} presented in [31] for $V_L = I$ turning on $V_L \simeq V_{\rm CKM}$, finding

$$\theta_{23} \lesssim \arctan\left[\frac{m_{\rm atm}\,s_{13}/\sqrt{2}}{(m_1+m_{\rm sol})\,c_{13}\,c_{12}\,s_{12} - V_{L12}\,(m_{\rm atm}-m_{\rm sol}-s_{12}^2\,m_1)/\sqrt{2}}\right] \sim 45^\circ\,, \tag{4.11}$$

where we took into account that $2\sigma - \delta \simeq -\pi/4$ and this yields the factor $1/\sqrt{2}$ in the numerator. In this case the largest angle θ_{12}^L gives the dominant effect.

[25] The reason why the peak of the asymmetry is just above the observed value is because we have deliberately chosen a solution at the border of the allowed region.

JHEP10(2017)029

We can also easily understand why the lower bound on m_{ee} gets strongly relaxed from $m_{ee} \gtrsim 1\,\text{meV}$ to $m_{ee} \gtrsim 0.1\,\text{meV}$ considering that

$$|\widetilde{m}_{\nu 11}| \simeq |\cos^2\theta^L_{12}\, m_{\nu ee} e^{i\,\rho_L} + \frac{1}{2}\sin 2\theta^L_{12}\, m_{\nu e\mu}|\,. \tag{4.12}$$

The lower bound $|m_{ee}| \gtrsim 1\,\text{meV}$ that was holding for $V_L = I$ translates now, for $V_L \simeq V_{\text{CKM}}$, into $|\widetilde{m}_{\nu 11}| \gtrsim 1\,\text{meV}$.[26] It is then possible to have the second term in $|\widetilde{m}_{\nu 11}|$ dominating and saturating the lower bound while $m_{\nu ee} \ll 1\,\text{meV}$. However, a lower bound still exists and m_{ee} cannot be arbitrary small. It is interesting actually to see from the panel in figure 1 showing m_{ee} versus δ, that there seems to be values of δ for which the lower bound becomes more stringent and that in any case the bulk of points is well above 1 meV and within reach of future experiments. This is an interesting feature of SO(10)-inspired leptogenesis. For the strong thermal points of course this is true even more stringently, since in this case $m_{ee} \gtrsim 10\,\text{meV}$ [23] and a signal should be in the reach of future experiments despite the fact that neutrino masses are NO.

We also want to remind, in conclusion of this subsection, that tauon-dominated solutions do not imply any fine-tuning in the seesaw formula, indeed the orthogonal matrix for these solutions has all entries $|\Omega_{ij}| \lesssim 1$, also for this reason they have then certainly to be regarded as the canonical and most attractive solutions.

4.3 Muon-dominated solutions

For $V_L = I$ there are no muon-dominated solutions [33]. In the *left panels* of figure 3 we show the dependence of different quantities on m_1 for $V_L = I$, $(\alpha_1, \alpha_2, \alpha_3) = (5, 5, 5)$ and for the indicated set of values of the low energy parameters. In particular one can notice how the *CP* flavoured asymmetries (second left panel from top) respect the strong hierarchical pattern in eq. (3.28) and even though both the wash-out at the production and, more importantly, from the lightest RH neutrino are negligible in the muon flavour, the final asymmetry (last left panel) falls many orders of magnitude below the observed value. Turning on $V_L \simeq V_{\text{CKM}}$, as we have seen in the scatter plots of figure 1, one does obtain muon-dominated solutions. We want to show here analytically how this occurs and derive an analytic expression that reproduces correctly the muon asymmetry.

First of all let us notice that the result in eq. (4.5) is well illustrated by the right panels of figure 3. They are obtained for the same set of values as in the left panels except that now $V_L \neq I$, with the only non-vanishing angle $\theta^L_{23} = 2.4^\circ \simeq \theta^{\text{CKM}}_{23}$ and also non-vanishing values of the phases σ_L and ρ_L. One can see that the muon asymmetry now gets enhanced compared to the right panel where $\theta^L_{23} = 0$ while the electron asymmetry is unchanged. This is in complete agreement with the result in eq. (4.5): for muon-dominated solutions it is then crucial to have non-vanishing θ^L_{23}.

The eq. (4.4) neglects a term $\propto |V_{L32}|^2$ that for a more accurate result we now need to add. Going back to the eq. (3.24), similarly to the tauon asymmetry, there are two terms

[26] This lower bound can be understood considering that $K_{1\tau} \propto |\widetilde{m}_{\nu 11}|^{-1}$ (see eq. (4.9)).

JHEP10(2017)029

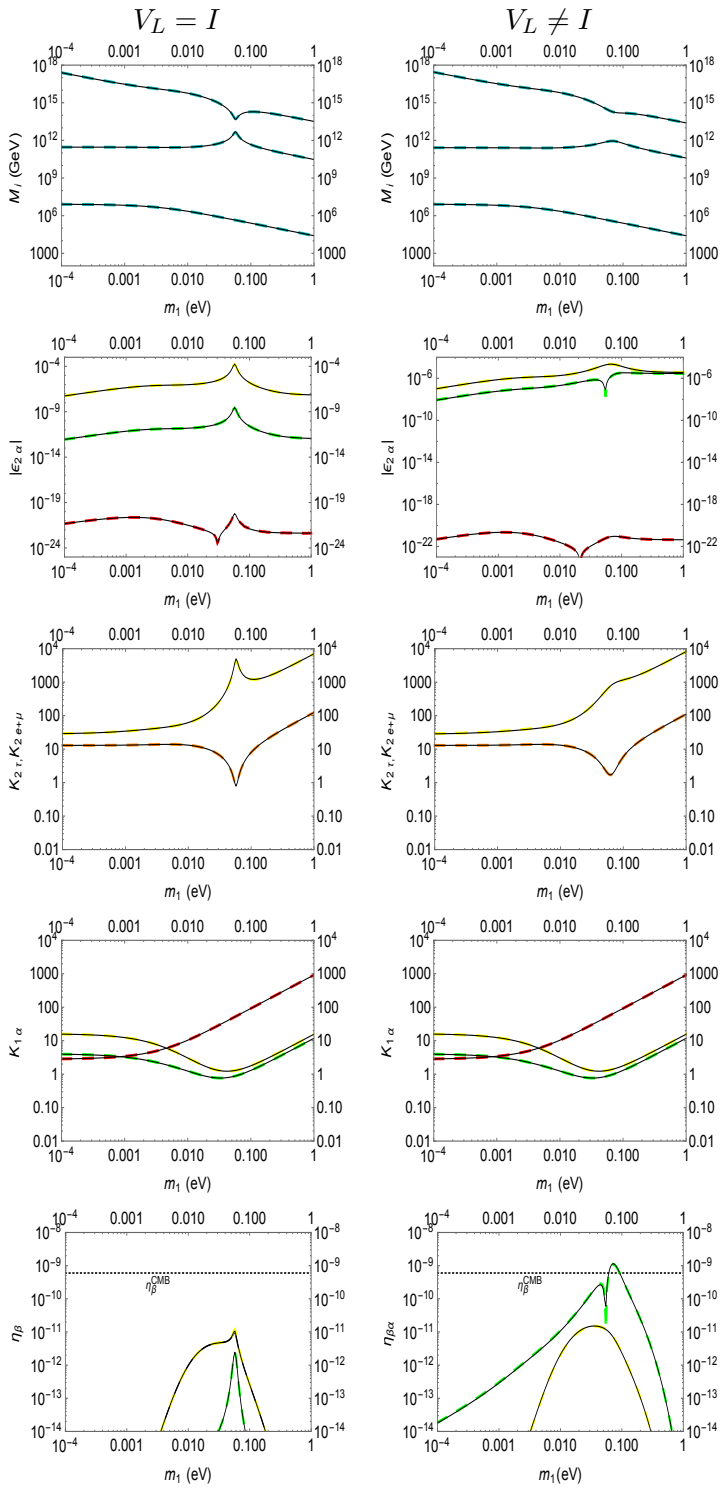

Figure 3. Example of muon-dominated solution. *Left panels*: $V_L = I$, $(\alpha_1, \alpha_2, \alpha_3) = (5, 5, 5)$, $(\theta_{13}, \theta_{12}, \theta_{23}) = (8.4°, 33°, 41°)$, $(\delta, \rho, \sigma) = (-0.3\pi, 0, 0.5\,\pi)$; *Right panels*: same as for left panels except that $\theta_{23}^L = 2.4°$ and $\sigma_L = -1.7\pi$ (the values of δ_L and ρ_L are irrelevant, since they cancel out for $\theta_{12}^L = \theta_{13}^L = 0$). All thin black lines are the analytical expressions for each quantity. The long-dashed coloured lines indicate the numerical results (same colour code as in figure 1: yellow for tauon flavour, green for muon flavour and red for electron flavour, the orange lines refer to the e+μ flavour).

JHEP10(2017)029

$\propto m_{D2}^2$ and one obtains

$$\varepsilon_{2\mu} \simeq \varepsilon_{2\mu}^{V_L} = \frac{3\, m_{D2}^2}{16\,\pi\, v^2}\, \frac{|(\widetilde{m}_\nu)_{11}|}{m_1\, m_2\, m_3} \times \frac{|(\widetilde{m}_\nu^{-1})_{23}|}{|(\widetilde{m}_\nu^{-1})_{33}|}\, \frac{|V_{L22}|\,|V_{L32}|\,\sin\alpha_L^{\mu A} + |V_{L32}|^2\,(|(\widetilde{m}_\nu^{-1})_{23}|/|(\widetilde{m}_\nu^{-1})_{33}|)\sin\alpha_L^{\mu B}}{|(\widetilde{m}_\nu^{-1})_{33}|^2 + |(\widetilde{m}_\nu^{-1})_{23}|^2}\,, \tag{4.13}$$

where

$$\alpha_L^{\mu A} = \mathrm{Arg}\,[\widetilde{m}_{\nu 11}] - \mathrm{Arg}[(\widetilde{m}_\nu^{-1})_{23}] - \mathrm{Arg}[(\widetilde{m}_\nu^{-1})_{33}] - 2\,(\rho+\sigma) - 2\,(\rho_L+\sigma_L)\,, \tag{4.14}$$

$$\alpha_L^{\mu B} = \mathrm{Arg}\,[\widetilde{m}_{\nu 11}] - 2\,\mathrm{Arg}[(\widetilde{m}_\nu^{-1})_{23}] - \pi - 2\,(\rho+\sigma) - 2\,(\rho_L+\sigma_L)\,. \tag{4.15}$$

This analytic expression for $\varepsilon_{2\mu}$ perfectly matches the numerical result in figure 2 (respectively the thin black line and the dashed green line). For completeness we also fit the muonic asymmetry for very small or vanishing θ_{23}^L, adding the following term ($\propto m_{D2}^4/m_{D3}^2$)

$$\varepsilon_{2\mu}^I \simeq \frac{3\, m_{D2}^2}{16\,\pi\, v^2}\, \frac{m_{D2}^2}{m_{D3}^2}\, \frac{|\widetilde{m}_{\nu 11}|}{m_1\, m_2\, m_3}\, \frac{|(\widetilde{m}_\nu^{-1})_{23}|^2}{|(\widetilde{m}_\nu^{-1})_{33}|^2}\, \frac{|V_{L22}|^2}{|(\widetilde{m}_\nu^{-1})_{33}|^2 + |(\widetilde{m}_\nu^{-1})_{23}|^2}\, \sin\widetilde{\alpha}_L\,, \tag{4.16}$$

where

$$\widetilde{\alpha}_L = \mathrm{Arg}\,[\widetilde{m}_{\nu 11}] - 2\,\mathrm{Arg}[(\widetilde{m}_\nu^{-1})_{23}] - 2\,(\rho+\sigma) - 2\,(\rho_L+\sigma_L)\,, \tag{4.17}$$

so that $\varepsilon_{2\mu} \simeq \varepsilon_{2\mu}^I + \varepsilon_{2\mu}^{V_L}$. Like in the limit $V_L \to I$, this term is not sufficiently large to reproduce the observed baryon asymmetry (not at least for $\alpha_2 \lesssim 5$), however by adding this term we could also reproduce $\varepsilon_{2\mu}$ in the case shown in figure 2, for a tauon-dominated solution.

One can also understand why muon-dominated solutions exist only in the range $0.01\,\mathrm{eV} \lesssim m_1 \lesssim 1\,\mathrm{eV}$ from the expressions eqs. (3.17) specialised for $K_{1\mu}$ and $K_{2\mu}$. In this case the deviations from $V_L = I$ give only corrections, as we will show explicitly, and we can first consider the simplified expressions for $V_L = I$. First of all we can write

$$K_{1\mu} = \frac{m_{D2}^2\,|U_{R21}|^2}{m_\star\, M_1} = \frac{|m_{\nu e\mu}|^2}{m_\star\, m_{ee}} = \frac{c_{13}^2\,\left|c_{12}\,s_{12}\,c_{23}\,(m_2 - m_1\,e^{2i\rho}) - s_{13}\,s_{23}\,e^{2i\sigma}\left[e^{i\delta}(m_1\,c_{12}^2 + m_2\,s_{12}^2) - m_3\,e^{-i\delta}\right]\right|^2}{m_\star\,|m_1\,c_{12}^2\,c_{13}^2\,e^{2i\rho} + m_2\,s_{12}^2\,c_{13}^2 + m_3\,s_{13}^2\,e^{i\,(2\sigma-\delta)}|}\,. \tag{4.18}$$

From this general expression one can easily see that in the hierarchical limit $m_1 \lesssim m_{\mathrm{sol}}$ one has

$$K_{1\mu} \to c_{12}^2\,c_{23}^2\,\frac{m_{\mathrm{sol}}}{m_\star} \simeq 3\,, \tag{4.19}$$

giving a too strong suppression in the hierarchical limit. On the other hand for $m_1 \gtrsim m_{\mathrm{sol}}$ one has $m_1 \simeq m_2$ and the dominant term in the numerator cancels out for $\rho \simeq n\,\pi$ and one can have $K_{1\mu} \lesssim 1$. However, for $m_1 \gtrsim m_{\mathrm{atm}}$, in the quasi-degenerate climit, one has

$$K_{1\mu} \to s_{23}^2\,s_{13}^2\,\frac{m_1}{m_\star}\left|1 - e^{2i(\sigma-\delta)}\right|^2\,. \tag{4.20}$$

JHEP10(2017)029

This can be still made small or even vanishing (for $\delta = \sigma$). The wash-out at the production is described by $K_{2\mu}$ (since $K_{2e} \lll K_{2\mu}$) given by

$$K_{2\mu} = \frac{m_{D2}^2}{m_\star\, M_2} = \frac{m_1\, m_2\, m_3 |(m_\nu^{-1})_{\tau\tau}|}{m_\star\, m_{ee}}\,, \tag{4.21}$$

that in the quasi-degenerate limit becomes

$$K_{2\mu} \to \frac{m_1}{m_\star}\, |s_{23}^2 + c_{23}^2\, c_{13}^2\, e^{-2i\sigma}|\,. \tag{4.22}$$

One can have a cancellation around $\sigma = (2m+1)\,\pi/2$ but away from this condition, for large values of m_1, $K_{2\mu}$ increases linearly with m_1. The larger is m_1, the sharper the conditions $\rho \simeq n\,\pi$ and $\delta = \sigma = (2k+1)\,\pi/2$ have to be satisfied. This can be clearly seen in the scatter plots in figure 1 (green points), while the linear increase of $K_{2\mu}$ with m_1 can be clearly seen in the example shown figure 2. However, the phase $\alpha_L \to 4\sigma$ in the quasi-degenerate limit and this leads to an upper bound on $m_1 \lesssim 1\,\text{eV}$, that however is quite relaxed compared to the corresponding one holding for tauon-dominated solutions discussed in detail in [31].

In the range $0.01\,\text{eV} \simeq m_{\text{sol}} \lesssim m_1 \lesssim 1\,\text{eV}$ one can have a strong reduction of $K_{2\mu}$ and $K_{1\mu} \lesssim 1$ and at the same time a sizeable CP asymmetry and this explains why in this range there are muon-dominated solutions that are now quite constrained by the current cosmological upper bound on m_1 and also by the upper bound on m_{ee} from $0\nu\beta\beta$ experiments.

In order to reproduce accurately the numerical results on the $K_{i\alpha}$'s vs. m_1 shown in the figure 2, one has to take into account corrections from $V_L \simeq V_{\text{CKM}}$, especially in the case of $K_{2\mu}$. We can first specialise the general expression eq. (3.17) writing

$$K_{2\mu} = \frac{m_1\, m_2\, m_3 |(\widetilde{m}_\nu^{-1})_{33}|}{m_\star\, \widetilde{m}_{\nu 11}} \sum_{k,l} V_{Lk\mu}\, V_{Ll\mu}^\star\, A_{k2}^\star\, A_{l2}\,, \tag{4.23}$$

and then we arrive to the approximate expression

$$\begin{aligned} K_{2\mu} \simeq & \frac{m_1\, m_2\, m_3 |(\widetilde{m}_\nu^{-1})_{33}|}{m_\star\, \widetilde{m}_{\nu 11}} \\ & \times \left(|V_{L22}|^2 + |V_{L12}|^2\, \frac{|\widetilde{m}_{\nu 12}|^2}{|\widetilde{m}_{\nu 11}|^2} + 2\, s_{23}^L\, \text{Re}\left[\frac{(\widetilde{m}_\nu^{-1})_{23}}{(\widetilde{m}_\nu^{-1})_{33}}\right] + |V_{L32}|^2\, \frac{|(\widetilde{m}_\nu^{-1})_{23}|^2}{|(\widetilde{m}_\nu^{-1})_{33}|^2} \right), \end{aligned} \tag{4.24}$$

that perfectly reproduces (thin black line) the numerical result (dashed orange line) both in figure 2 and in figure 3. We also derived an analogous expression for $K_{1\mu}$ also reproducing the numerical results in figure 2 and in figure 3.

There is another important aspect to be reported of muon-dominated solutions: they necessarily rely on some amount of fine tuning in the seesaw formula as it can be understood from the expression of the orthogonal matrix eq. (3.11). These solutions exist for values of the parameters about the crossing level solution where $M_2 = M_3$. Even though one still has $M_3 \gg M_2$, the value of M_2 gets enhanced and correspondingly the value of $\varepsilon_{2\mu}$, this is clearly visible in the panels of figure 3. This possibility relies on the value of $(\widetilde{m}_\nu^{-1})_{33}$ in

JHEP10(2017)029

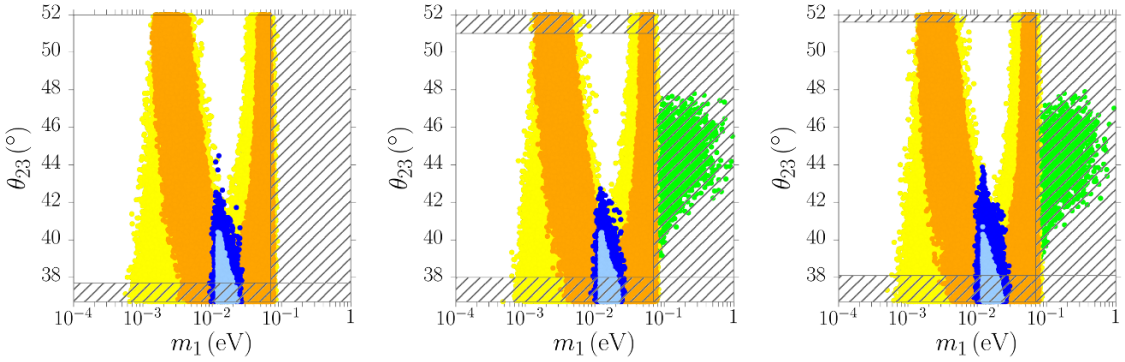

Figure 4. Scatter plots in the plane θ_{23} versus m_1 as in figure 1 but for $M_\Omega = 3, 10, 100$ from left to right.

the denominator of M_2 to get reduced thanks to some mild phase cancellation. By itself this is not a problem, however for small values of $(\widetilde{m}_\nu^{-1})_{33}$ the second and third column in the orthogonal matrix get correspondingly enhanced, as it can be seen from eq. (3.11) and this necessarily implies a fine tuning in the seesaw formula at the level of $1/|\Omega|^2_{ij}$. These analytical considerations are fully confirmed by the scatter plots obtained numerically. In figure 4 in the left panel we compare scatter plots of solutions in the plane θ_{23} vs. m_1 imposing the condition $|\Omega_{ij}|^2 < 3, 10, 100$ from left to right: one can notice how in the first case all muon-dominated solutions, those at values $m_1 \gtrsim 0.01\,\text{eV}$, completely disappear. From this point of view it should be clear that tauon-dominated solutions, the bulk of solutions within SO(10)-inspired leptogenesis, are the only completely untuned solutions.[27]

4.4 Electron-dominated solutions?

In the scatter plots shown in figure 1, for $M_\Omega < 100$ and $M_3 \geq 2\,M_2$, we could not find any electron-dominated solution.[28] From the results in eq. (3.28) and eq. (4.5) we can understand the reason: for $V_L = I$ the electron CP asymmetry is suppressed by more than 15 orders of magnitude compared to the tauonic CP asymmetry and even turning on $V_L \simeq V_{\rm CKM}$ is not enough since ε_{2e} is still suppressed $\propto \theta^L_{13}\,\theta^L_{12}$ compared to the tauonic CP asymmetry $\varepsilon_{2\tau}$.

It is however still worth to give briefly analytic expressions for the three quantities $(\varepsilon_{2e}, K_{1e}, K_{2e})$ involved in the calculation of the electronic contribution to the asymmetry.

[27] Indeed constraints in figure 4 do not change increasing M_Ω for tauon-dominated solutions (yellow and orange points).

[28] The maximum asymmetry that an electron dominated solution can produce is $\eta_B \simeq 3\times 10^{-10}$ for values $m_1 \simeq 4\,\text{meV}$ corresponding to have $(\widetilde{m}_\nu^{-1})_{33}$ very small, in the vicinity of the crossing level $M_2 \simeq M_3$. These solutions involve, as stressed already a few times, a high fine tuning in the seesaw formula. The value of M_2 is necessarily capped below $10^{12}\,\text{GeV}$ since if it goes above, though the CP asymmetry would grow, the wash-out at the production would occur in the unflavoured regime experiencing a very strong wash-out due to a huge value of $K_{2\tau} \simeq K_2$. In the supersymmetric case the double value of the CP asymmetries and the fact that the transition to the unflavoured regime occurs at higher values $M_2 \simeq 10^{12}\,\text{GeV}\,(1+\tan^2\beta)$, conspire in a way that sparse (very fine-tuned) electronic solutions do appear.

JHEP10(2017)029

The reason is that they can be easily extended to models or frameworks where there might be some enhancement. For example either in SO(10)-inspired models that, for some reason, have a large θ_{13}^L, or to a supersymmetric framework where the *CP* asymmetry doubles and the wash-out at the production can occur in the three-flavoured regime and be greatly reduced and in both these cases one can have the appearance of electron-dominated solutions. The third reason is that in this way we can extend our analytic description and show agreement with the numerical results in the two examples of figure 2 and figure 3 also for the quantities in the electron flavour (K_{1e}, K_{2e}, ε_{2e}, $\eta_B^{(e)}$). This is not just an aesthetic reason but it provides yet another cross check making us confident of the accuracy of our analytic solution.

Analogously to $\varepsilon_{2\mu}$ the electron *CP* asymmetry can also be written as the sum of two terms,

$$\varepsilon_{2e} = \varepsilon_{2e}^{I} + \varepsilon_{2e}^{V_L} \,. \tag{4.25}$$

The first one is the non-vanishing one in the limit for $V_L \to I$ and is very strongly suppressed[29] and given by

$$\varepsilon_{2e}^{I} = \frac{3\, m_{D2}^2}{16\,\pi\, v^2}\, \frac{m_{D1}^4}{m_{D2}^4}\, \frac{m_{D2}^2}{m_{D3}^2}\, \frac{|\widetilde{m}_{\nu 12}|}{m_1\, m_2\, m_3}\, \frac{|(\widetilde{m}_\nu^{-1})_{13}|\, |(\widetilde{m}_\nu^{-1})_{23}|}{|(\widetilde{m}_\nu^{-1})_{33}|^2}\, \frac{|V_{L11}|^2}{|(\widetilde{m}_\nu^{-1})_{33}|^2 + |(\widetilde{m}_\nu^{-1})_{23}|^2}\, \sin\widetilde{\alpha}_{Le}^{I} \,, \tag{4.26}$$

with

$$\widetilde{\alpha}_{Le}^{I} = \mathrm{Arg}\,[\widetilde{m}_{\nu 12}] - \mathrm{Arg}[(\widetilde{m}_\nu^{-1})_{23}] - \mathrm{Arg}[(\widetilde{m}_\nu^{-1})_{13}] - \pi - 2\,(\rho+\sigma) - 2\,(\rho_L+\sigma_L) \,. \tag{4.27}$$

The second one dominates when $V_L \simeq V_{\rm CKM}$ and is given by

$$\varepsilon_{2e}^{V_L} = \frac{3\, m_{D2}^2}{16\,\pi\, v^2}\, \frac{|\widetilde{m}_{\nu 11}|}{m_1\, m_2\, m_3}\, \frac{|(\widetilde{m}_\nu^{-1})_{23}|}{|(\widetilde{m}_\nu^{-1})_{33}|}\, \frac{|V_{L21}|\, |V_{L31}|}{|(\widetilde{m}_\nu^{-1})_{33}|^2 + |(\widetilde{m}_\nu^{-1})_{23}|^2}\, \sin\widetilde{\alpha}_{Le}^{I} \,, \tag{4.28}$$

with $\widetilde{\alpha}_{Le}^{I} = \alpha_{L\mu}^{A}$. For the flavoured decay parameters the following expressions accurately reproduce the numerical results

$$K_{1e} \simeq \frac{|\widetilde{m}_{\nu 11}|}{m_\star}\, \left(|V_{L11}|^2 - 2\,|V_{L11}|\,|V_{L21}|\,\mathrm{Re}[\widetilde{m}_{\nu 12}/\widetilde{m}_{\nu 11}] + |V_{L21}|^2\, |\widetilde{m}_{\nu 12}|^2/|\widetilde{m}_{\nu 11}|^2\right) \,, \tag{4.29}$$

while for all purposes K_{2e} can be completely neglected in the wash-out at the production, thus entirely dominated by $K_{2\mu}$. We conclude this subsection mentioning that in [39] electronic solutions had been found including a term in the asymmetry generated by flavour coupling. However these solutions require strong fine-tuning in the seesaw formula at the level of 0.1%.

5 Conclusions

We obtained a full analytical description for the calculation of the baryon asymmetry in SO(10)-inspired leptogenesis,[30] generalising the results obtained in [31] accounting for the

[29] We are including it simply to describe ε_{2e} correctly even when $V_L \to I$.

[30] The set of analytical expressions are summarised in the appendix.

JHEP10(2017)029

misalignment between the Yukawa basis and the flavour basis described by a unitary matrix with mixing angles at the level of the mixing angles in the CKM matrix in the quark sector. In this way we could provide an analytical insight into SO(10)-inspired leptogenesis able to explain the relaxation of constraints, in particular the upper bound on the atmospheric mixing angles in the case of strong thermal (tauon-dominated) solutions and the appearance of muon-dominated solutions at large values of $m_1 \gtrsim m_{\rm sol}$. We have shown how the analytic solution we obtained does not just provide a qualitative understanding, but in fact, within the given set of assumption, it reproduces accurately the asymmetry calculated numerically and can be basically confidently used for the calculation of the baryon asymmetry in SO(10)-inspired leptogenesis without passing through the lengthy numerical diagonalisation of the Majorana mass matrix in the Yukawa basis. This solution provides a thorough analytic insight and paves the way for the account of different effects in the derivation of the constraints on the low energy neutrino parameters, including, importantly, their statistical significance, a crucial step in light of the expected future experimental progress, for the testability of SO(10)-inspired leptogenesis.

Acknowledgments

PDB acknowledges financial support from the NExT/SEPnet Institute. PDB acknowledges financial support from the STFC Consolidated Grant ST/L000296/1. This project has received funding from the European Union's Horizon 2020 research and innovation programme under the Marie Sklodowska-Curie grant agreement No 690575 and No 674896. PDB is also grateful to the Tokyo University for its hospitality during the period this paper was prepared and wishes to thank Koichi Hamaguchi for useful discussions.

A Compendium

In this appendix we summarise in a compact way all the set of analytical expressions that constitute the solution of SO(10)-inspired leptogenesis we found. This set can be easily plugged in to a simple code for a fast calculation of the asymmetry and the generation of a big amount of solutions. This is the set of needed equations:

$$\widetilde{m}_\nu \equiv V_L \, m_\nu \, V_L^T \,, \tag{A.1}$$

$$\Phi_1 = \mathrm{Arg}\left[-\widetilde{m}^\star_{\nu 11}\right] \,, \tag{A.2}$$

$$\Phi_2 = \mathrm{Arg}\left[\frac{\widetilde{m}_{\nu 11}}{(\widetilde{m}_\nu^{-1})_{33}}\right] - 2\,(\rho+\sigma) - 2\,(\rho_L+\sigma_L)\,, \tag{A.3}$$

$$\Phi_3 = \mathrm{Arg}\left[-(\widetilde{m}_\nu^{-1})_{33}\right] \,, \tag{A.4}$$

$$D_\phi \equiv \mathrm{diag}\left(e^{-i\frac{\Phi_1}{2}}, e^{-i\frac{\Phi_2}{2}}, e^{-i\frac{\Phi_3}{2}}\right) \,, \tag{A.5}$$

JHEP10(2017)029

$$U_R \simeq \begin{pmatrix} 1 & -\frac{m_{D1}}{m_{D2}}\frac{\widetilde{m}^\star_{\nu 12}}{\widetilde{m}^\star_{\nu 11}} & \frac{m_{D1}}{m_{D3}}\frac{(\widetilde{m}_\nu^{-1})^\star_{13}}{(\widetilde{m}_\nu^{-1})^\star_{33}} \\ \frac{m_{D1}}{m_{D2}}\frac{\widetilde{m}_{\nu 12}}{\widetilde{m}_{\nu 11}} & 1 & \frac{m_{D2}}{m_{D3}}\frac{(\widetilde{m}_\nu^{-1})^\star_{23}}{(\widetilde{m}_\nu^{-1})^\star_{33}} \\ \frac{m_{D1}}{m_{D3}}\frac{\widetilde{m}_{\nu 13}}{\widetilde{m}_{\nu 11}} & -\frac{m_{D2}}{m_{D3}}\frac{(\widetilde{m}_\nu^{-1})_{23}}{(\widetilde{m}_\nu^{-1})_{33}} & 1 \end{pmatrix} D_\Phi \,, \tag{A.6}$$

$$M_1 \simeq \frac{\alpha_1^2\, m_{\rm u}^2}{|(\widetilde{m}_\nu)_{11}|}\,, \tag{A.7}$$

$$M_2 \simeq \frac{\alpha_2^2\, m_{\rm c}^2}{m_1\, m_2\, m_3}\,\frac{|(\widetilde{m}_\nu)_{11}|}{|(\widetilde{m}_\nu^{-1})_{33}|}\,, \tag{A.8}$$

$$M_3 \simeq \alpha_3^2\, m_{\rm t}^2\, |(\widetilde{m}_\nu^{-1})_{33}|\,, \tag{A.9}$$

$$K_{i\alpha} = \frac{\sum_{k,l}\, m_{Dk}\, m_{Dl}\, V_{Lk\alpha}\, V^\star_{Ll\alpha}\, U^\star_{Rki}\, U_{Rli}}{M_i\, m_\star}\,, \tag{A.10}$$

$$\varepsilon_{2\alpha} \simeq \frac{3}{16\,\pi\, v^2}\,\frac{|(\widetilde{m}_\nu)_{11}|}{m_1\, m_2\, m_3}\,\frac{\sum_{k,l}\, m_{Dk}\, m_{Dl}\, {\rm Im}[V_{Lk\alpha}\, V^\star_{Ll\alpha}\, U^\star_{Rk2}\, U_{Rl3}\, U^\star_{R32}\, U_{R33}]}{|(\widetilde{m}_\nu^{-1})_{33}|^2 + |(\widetilde{m}_\nu^{-1})_{23}|^2}\,, \tag{A.11}$$

$$N^{\rm lep,f}_{\Delta_e} \simeq \varepsilon_{2e}\, \kappa(K_{2e} + K_{2\mu})\, e^{-\frac{3\pi}{8} K_{1e}}\,, \tag{A.12}$$

$$N^{\rm lep,f}_{\Delta_\mu} \simeq \varepsilon_{2\mu}\, \kappa(K_{2e} + K_{2\mu})\, e^{-\frac{3\pi}{8} K_{1\mu}}\,, \tag{A.13}$$

$$N^{\rm lep,f}_{\Delta_\tau} \simeq \varepsilon_{2\tau}\, \kappa(K_{2\tau})\, e^{-\frac{3\pi}{8} K_{1\tau}}\,, \tag{A.14}$$

$$N^{\rm p,f}_{B-L} = \sum_\alpha N^{\rm p,f}_{\Delta_\alpha}\,, \tag{A.15}$$

and finally

$$\eta^{\rm lep}_B = a_{\rm sph}\,\frac{N^{\rm lep,f}_{B-L}}{N^{\rm rec}_\gamma} \simeq 0.96\times 10^{-2}\, N^{\rm lep,f}_{B-L}\,. \tag{A.16}$$

Notice that all these expressions are valid for any V_L, it indeed relies only on the first assumption of SO(10)-inspired leptogenesis (hierarchical Yukawas) and not on the second, small angles in V_L. This can be checked easily simply taking as an example the extreme case when all leptonic mixing comes from V_L, in a way that $V_L = U^\dagger$ and $U_R = I$. In this case simply $\widetilde{m_\nu} = -D_m$ and simply $M_1 = m^2_{D1}/m_1$, $M_2 = m^2_{D2}/m_2$ and $M_3 = m^2_{D3}/m_3$, as it has to be considering that $\Omega = I$. One can indeed also check that the analytic expression for the Ω matrix eq. (3.11) reduces to $\Omega = I$. This shows that the analytical expressions are consistent with a choice of V_L that is very different from $V_L \simeq V_{\rm CKM}$. Notice, however, that in this case it is not guaranteed that $M_1 \lesssim 10^9\,{\rm GeV}$ and so that the N_2-dominated scenario of leptogenesis holds. For this one needs also to impose $I \leq V_L \lesssim V_{\rm CKM}$. For small mixing angles θ^L_{ij} one can extract the leading terms in the sums in eqs. (A.10) and (A.11) obtaining the explicit analytic expressions we showed in the body text and that we do not repeat here.

JHEP10(2017)029

References

[1] I. Shipsey, *Vision and Outlook from Quark to the Cosmos*, concluding talk at *ICHEP 2016*, PoS(ICHEP2016)037, https://indico.cern.ch/event/432527/contributions/2220326/attachments/1322666/1984227/ICHEP-Vision-Outlook-v4-b.pdf.

[2] P. Minkowski, $\mu \to e\gamma$ *at a Rate of One Out of* 10^9 *Muon Decays?*, *Phys. Lett.* **B 67** (1977) 421 [INSPIRE].

[3] T. Yanagida, *Horizontal symmetry and masses of neutrinos*, in *Proceedings of the Workshop on Unified Theory and Baryon Number of the Universe*, O. Sawada and A. Sugamoto eds., KEK, (1979), p. 95.

[4] P. Ramond, *The Family Group in Grand Unified Theories*, CALT-68-709, hep-ph/9809459 [INSPIRE].

[5] M. Gell-Mann, P. Ramond and R. Slansky, *Complex Spinors and Unified Theories*, in *Supergravity*, P. van Niewwenhuizen and D. Freedman eds., North Holland, Amsterdam, The Netherlands (1979), *Conf. Proc.* **C 790927** (1979) 315 [arXiv:1306.4669] [INSPIRE].

[6] R. Barbieri, D.V. Nanopoulos, G. Morchio and F. Strocchi, *Neutrino Masses in Grand Unified Theories*, *Phys. Lett.* **B 90** (1980) 91 [INSPIRE].

[7] R.N. Mohapatra and G. Senjanović, *Neutrino Mass and Spontaneous Parity Violation*, *Phys. Rev. Lett.* **44** (1980) 912 [INSPIRE].

[8] M. Fukugita and T. Yanagida, *Baryogenesis Without Grand Unification*, *Phys. Lett.* **B 174** (1986) 45 [INSPIRE].

[9] F. Capozzi, E. Di Valentino, E. Lisi, A. Marrone, A. Melchiorri and A. Palazzo, *Global constraints on absolute neutrino masses and their ordering*, *Phys. Rev.* **D 95** (2017) 096014 [arXiv:1703.04471] [INSPIRE].

[10] I. Esteban, M.C. Gonzalez-Garcia, M. Maltoni, I. Martinez-Soler and T. Schwetz, *Updated fit to three neutrino mixing: exploring the accelerator-reactor complementarity*, *JHEP* **01** (2017) 087 [arXiv:1611.01514] [INSPIRE].

[11] W. Buchmüller, P. Di Bari and M. Plümacher, *A bound on neutrino masses from baryogenesis*, *Phys. Lett.* **B 547** (2002) 128 [hep-ph/0209301] [INSPIRE].

[12] W. Buchmüller, P. Di Bari and M. Plümacher, *The neutrino mass window for baryogenesis*, *Nucl. Phys.* **B 665** (2003) 445 [hep-ph/0302092] [INSPIRE].

[13] W. Buchmüller, P. Di Bari and M. Plümacher, *Leptogenesis for pedestrians*, *Annals Phys.* **315** (2005) 305 [hep-ph/0401240] [INSPIRE].

[14] G.F. Giudice, A. Notari, M. Raidal, A. Riotto and A. Strumia, *Towards a complete theory of thermal leptogenesis in the SM and MSSM*, *Nucl. Phys.* **B 685** (2004) 89 [hep-ph/0310123] [INSPIRE].

[15] A. De Simone and A. Riotto, *On the impact of flavour oscillations in leptogenesis*, *JCAP* **02** (2007) 005 [hep-ph/0611357] [INSPIRE].

[16] S. Blanchet and P. Di Bari, *New aspects of leptogenesis bounds*, *Nucl. Phys.* **B 807** (2009) 155 [arXiv:0807.0743] [INSPIRE].

JHEP10(2017)029

[17] E. Nardi, Y. Nir, E. Roulet and J. Racker, *The importance of flavor in leptogenesis*, *JHEP* **01** (2006) 164 [hep-ph/0601084] [INSPIRE].

[18] A. Abada, S. Davidson, A. Ibarra, F.X. Josse-Michaux, M. Losada and A. Riotto, *Flavour Matters in Leptogenesis*, *JHEP* **09** (2006) 010 [hep-ph/0605281] [INSPIRE].

[19] P. Di Bari, *Seesaw geometry and leptogenesis*, *Nucl. Phys.* **B 727** (2005) 318 [hep-ph/0502082] [INSPIRE].

[20] NOvA collaboration, P. Adamson et al., *Measurement of the neutrino mixing angle θ_{23} in NOvA*, *Phys. Rev. Lett.* **118** (2017) 151802 [arXiv:1701.05891] [INSPIRE].

[21] T2K collaboration, K. Abe et al., *Combined Analysis of Neutrino and Antineutrino Oscillations at T2K*, *Phys. Rev. Lett.* **118** (2017) 151801 [arXiv:1701.00432] [INSPIRE].

[22] IceCube collaboration, J.P.A.M. de Andrè, *Recent Results from IceCube neutrino oscillations*, talk at *52nd Rencontres de Moriond EW*, La Thuile, Italy, 18–25 March 2017.

[23] P. Di Bari and L. Marzola, SO(10)*-inspired solution to the problem of the initial conditions in leptogenesis*, *Nucl. Phys.* **B 877** (2013) 719 [arXiv:1308.1107] [INSPIRE].

[24] P. Di Bari and L. Marzola, *Testing New Physics with Leptogenesis*, talks at the *DESY theory workshop on Cosmology meets particles*, September 2011, http://th-workshop2011.desy.de/.

[25] A. Yu. Smirnov, *Seesaw enhancement of lepton mixing*, *Phys. Rev.* **D 48** (1993) 3264 [hep-ph/9304205] [INSPIRE].

[26] W. Buchmüller and M. Plümacher, *Baryon asymmetry and neutrino mixing*, *Phys. Lett.* **B 389** (1996) 73 [hep-ph/9608308] [INSPIRE].

[27] E. Nezri and J. Orloff, *Neutrino oscillations versus leptogenesis in* SO(10) *models*, *JHEP* **04** (2003) 020 [hep-ph/0004227] [INSPIRE].

[28] F. Buccella, D. Falcone and F. Tramontano, *Baryogenesis via leptogenesis in* SO(10) *models*, *Phys. Lett.* **B 524** (2002) 241 [hep-ph/0108172] [INSPIRE].

[29] G.C. Branco, R. Gonzalez Felipe, F.R. Joaquim and M.N. Rebelo, *Leptogenesis, CP-violation and neutrino data: What can we learn?*, *Nucl. Phys.* **B 640** (2002) 202 [hep-ph/0202030] [INSPIRE].

[30] E. Bertuzzo, P. Di Bari and L. Marzola, *The problem of the initial conditions in flavoured leptogenesis and the tauon N_2-dominated scenario*, *Nucl. Phys.* **B 849** (2011) 521 [arXiv:1007.1641] [INSPIRE].

[31] P. Di Bari, L. Marzola and M. Re Fiorentin, *Decrypting* SO(10)*-inspired leptogenesis*, *Nucl. Phys.* **B 893** (2015) 122 [arXiv:1411.5478] [INSPIRE].

[32] P. Di Bari and M. Re Fiorentin, *Supersymmetric* SO(10)*-inspired leptogenesis and a new N_2-dominated scenario*, *JCAP* **03** (2016) 039 [arXiv:1512.06739] [INSPIRE].

[33] P. Di Bari and A. Riotto, *Testing* SO(10)*-inspired leptogenesis with low energy neutrino experiments*, *JCAP* **04** (2011) 037 [arXiv:1012.2343] [INSPIRE].

[34] Planck collaboration, P.A.R. Ade et al., *Planck 2015 results. XIII. Cosmological parameters*, *Astron. Astrophys.* **594** (2016) A13 [arXiv:1502.01589] [INSPIRE].

[35] KamLAND-Zen collaboration, A. Gando et al., *Search for Majorana Neutrinos near the Inverted Mass Hierarchy Region with KamLAND-Zen*, *Phys. Rev. Lett.* **117** (2016) 082503 *Addendum ibid.* **117** (2016) 109903 [arXiv:1605.02889] [INSPIRE].

[36] E.K. Akhmedov, M. Frigerio and A.Yu. Smirnov, *Probing the seesaw mechanism with neutrino data and leptogenesis*, *JHEP* **09** (2003) 021 [hep-ph/0305322] [INSPIRE].

JHEP10(2017)029

[37] J.A. Casas and A. Ibarra, *Oscillating neutrinos and muon* $\to e, \gamma$, *Nucl. Phys.* **B 618** (2001) 171 [hep-ph/0103065] [INSPIRE].

[38] P. Di Bari and A. Riotto, *Successful type-I Leptogenesis with* SO(10)*-inspired mass relations*, *Phys. Lett.* **B 671** (2009) 462 [arXiv:0809.2285] [INSPIRE].

[39] P. Di Bari and S.F. King, *Successful* N_2 *leptogenesis with flavour coupling effects in realistic unified models*, *JCAP* **10** (2015) 008 [arXiv:1507.06431] [INSPIRE].

[40] S. Yu. Khlebnikov and M.E. Shaposhnikov, *The Statistical Theory of Anomalous Fermion Number Nonconservation*, *Nucl. Phys.* **B 308** (1988) 885 [INSPIRE].

[41] J.A. Harvey and M.S. Turner, *Cosmological baryon and lepton number in the presence of electroweak fermion number violation*, *Phys. Rev.* **D 42** (1990) 3344 [INSPIRE].

[42] P. Di Bari, S. King and M. Re Fiorentin, *Strong thermal leptogenesis and the absolute neutrino mass scale*, *JCAP* **03** (2014) 050 [arXiv:1401.6185] [INSPIRE].

[43] O. Vives, *Flavor dependence of CP asymmetries and thermal leptogenesis with strong right-handed neutrino mass hierarchy*, *Phys. Rev.* **D 73** (2006) 073006 [hep-ph/0512160] [INSPIRE].

[44] S. Antusch, P. Di Bari, D.A. Jones and S.F. King, *A fuller flavour treatment of* N_2*-dominated leptogenesis*, *Nucl. Phys.* **B 856** (2012) 180 [arXiv:1003.5132] [INSPIRE].

[45] S. Blanchet, P. Di Bari, D.A. Jones and L. Marzola, *Leptogenesis with heavy neutrino flavours: from density matrix to Boltzmann equations*, *JCAP* **01** (2013) 041 [arXiv:1112.4528] [INSPIRE].

[46] S. Davidson and A. Ibarra, *A lower bound on the right-handed neutrino mass from leptogenesis*, *Phys. Lett.* **B 535** (2002) 25 [hep-ph/0202239] [INSPIRE].

[47] S. Blanchet and P. Di Bari, *Flavor effects on leptogenesis predictions*, *JCAP* **03** (2007) 018 [hep-ph/0607330] [INSPIRE].

[48] D. Bödeker and M. Wörmann, *Non-relativistic leptogenesis*, *JCAP* **02** (2014) 016 [arXiv:1311.2593] [INSPIRE].

[49] L. Covi, E. Roulet and F. Vissani, *CP violating decays in leptogenesis scenarios*, *Phys. Lett.* **B 384** (1996) 169 [hep-ph/9605319] [INSPIRE].

[50] H. Fusaoka and Y. Koide, *Updated estimate of running quark masses*, *Phys. Rev.* **D 57** (1998) 3986 [hep-ph/9712201] [INSPIRE].

[51] A. Dueck and W. Rodejohann, *Fits to* SO(10) *Grand Unified Models*, *JHEP* **09** (2013) 024 [arXiv:1306.4468] [INSPIRE].

[52] F. Buccella, D. Falcone, C.S. Fong, E. Nardi and G. Ricciardi, *Squeezing out predictions with leptogenesis from* SO(10), *Phys. Rev.* **D 86** (2012) 035012 [arXiv:1203.0829] [INSPIRE].

[53] P. Di Bari and M. Re Fiorentin, in preparation.

[54] S. Blanchet, D. Marfatia and A. Mustafayev, *Examining leptogenesis with lepton flavor violation and the dark matter abundance*, *JHEP* **11** (2010) 038 [arXiv:1006.2857] [INSPIRE].

JHEP10(2017)029